Cellular/Molecular

PKC Enhances the Capacity for Secretion by Rapidly Recruiting Covert Voltage-Gated Ca^{2+} Channels to the Membrane

Christopher J. Groten and Neil S. Magoski
Department of Biomedical and Molecular Sciences, Physiology Graduate Program, Queen's University, Kingston, Ontario K7L3N6, Canada

It is unknown whether neurons can dynamically control the capacity for secretion by promptly changing the number of plasma membrane voltage-gated Ca^{2+} channels. To address this, we studied peptide release from the bag cell neurons of *Aplysia californica*, which initiate reproduction by secreting hormone during an afterdischarge. This burst engages protein kinase C (PKC) to trigger the insertion of a covert Ca^{2+} channel, Apl Ca_v2, alongside a basal channel, Apl Ca_v1. The significance of Apl Ca_v2 recruitment to secretion remains undetermined; therefore, we used capacitance tracking to assay secretion, along with Ca^{2+} imaging and Ca^{2+} current measurements, from cultured bag cell neurons under whole-cell voltage-clamp. Activating PKC with the phorbol ester, PMA, enhanced Ca^{2+} entry, and potentiated stimulus-evoked secretion. This relied on channel insertion, as it was occluded by preventing Apl Ca_v2 engagement with prior whole-cell dialysis or the cytoskeletal toxin, latrunculin B. Channel insertion reduced the stimulus duration and/or frequency required to initiate secretion and strengthened excitation-secretion coupling, indicating that Apl Ca_v2 accesses peptide release more readily than Apl Ca_v1. The coupling of Apl Ca_v2 to secretion also changed with behavioral state, as Apl Ca_v2 failed to evoke secretion in silent neurons from reproductively inactive animals. Finally, PKC also acted secondarily to enhance prolonged exocytosis triggered by mitochondrial Ca^{2+} release. Collectively, our results suggest that bag cell neurons dynamically elevate Ca^{2+} channel abundance in the membrane to ensure adequate secretion during the afterdischarge.

Key words: *Aplysia*; bag cell neurons; Ca^{2+} channel insertion; mitochondria; peptide secretion; PMA

Introduction

Neurons and neuroendocrine cells can enter states of heightened activity and secretory capacity underlying fundamental processes, such as synaptic facilitation and high-threshold hormone release. Protein kinases, including protein kinase C (PKC), A (PKA), and calmodulin kinase, often mediate these transitions by regulating the activity of voltage-gated Ca^{2+} channels (Artalejo et al., 1994; Catterall, 2000; Catterall and Few, 2008). Typically, kinases modulate Ca^{2+} current by directly regulating ion channels residing in the plasma membrane. Alternatively, kinases can elevate macroscopic current by inducing the insertion of additional channels into the membrane. Rapid channel recruitment underlies various forms of plasticity, including plateau potentials mediated by TRP channels and LTP involving AMPA receptors (Man et al., 2003; Tai et al., 2011). As Ca^{2+} channel abundance determines synaptic strength (Hoppa et al., 2012; Sheng et al., 2012), analogous kinase-dependent changes to membrane Ca^{2+} channels could provide an effective means for neurons to control secretory capability. Although augmented Ca^{2+} channel trafficking/insertion has been implicated in regulating synaptic transmission, this requires a period of hour to days (Bauer et al., 2009; Hendrich et al., 2012). Therefore, it remains unknown whether neurons can use a dynamic Ca^{2+} channel pool to quickly boost output on a time scale of minutes.

A well studied and unique model of Ca^{2+} channel insertion is found in the bag cell neurons of the marine mollusc, *Aplysia californica*. Following a brief synaptic input, these neuroendocrine cells transition from quiescence to a period of prolonged activity, known as the afterdischarge, to release egg-laying hormone (ELH) and trigger reproduction (Kupfermann, 1967; Kupfermann and Kandel, 1970; Arch, 1972; Pinsker and Dudek, 1977). Shortly after the start of the afterdischarge, PKC is stimulated, and enhances Ca^{2+} current via the insertion of a covert, larger-conductance Ca^{2+} channel, termed Apl Ca_v2, alongside the constitutively present, smaller-conductance channel, termed Apl Ca_v1 (Strong et al., 1987; Conn et al., 1989b; Wayne et al., 1999). Immunocytochemistry and membrane protein biotinylation assays show that the ion conducting α-1 subunit of Apl Ca_v2 is exclusively localized to intracellular vesicles under resting conditions, but upon PKC activation, it associates with actin and inserts into the plasma membrane of the soma and neurites (White and Kaczmarek, 1997; White et al., 1998; Zhang et al., 2008).

Received Aug. 25, 2014; revised Dec. 16, 2014; accepted Jan. 1, 2015.
Author contributions: C.J.G. and N.S.M. designed research; C.J.G. performed research; C.J.G. and N.S.M. analyzed data; C.J.G. and N.S.M. wrote the paper.
This work was supported by a CIHR operating grant (N.S.M.). C.J.G. holds an NSERC Postgraduate Doctoral Scholarship. We thank H.M. Hodgson for technical assistance.
The authors declare no competing financial interests.
Correspondence should be addressed to Dr Neil S. Magoski, Queen's University, Department of Biomedical and Molecular Sciences, 4th Floor, Botterell Hall, 18 Stuart Street, Kingston, ON, K7L 3N6, Canada. E-mail: magoski@queensu.ca.
DOI:10.1523/JNEUROSCI.3581-14.2015
 0270-6474/15/352747-19$15.00/0

The physiological implications of Apl Ca_v2 insertion on secretion remain undetermined. In the present study, we dissected the effects of PKC and Apl Ca_v2 insertion on evoked secretion by using capacitance tracking and Ca^{2+} imaging in cultured bag cell neurons. We show that Apl Ca_v2 strongly augments stimulus-evoked Ca^{2+} entry and secretion, while also strengthening excitation-secretion coupling. Furthermore, through a mechanism downstream from Ca^{2+} influx, PKC activation enhances prolonged exocytosis triggered by slow intracellular Ca^{2+} release from mitochondria. These results suggest that the bag cell neurons use Apl Ca_v2 to transform the secretory capacity of bag cell neurons during the afterdischarge. To our knowledge, the present findings are the first to demonstrate that neurons can dynamically amplify output by rapidly recruiting additional voltage-gated Ca^{2+} channels to the membrane.

Materials and Methods

Animals and cell culture. Adult *Aplysia californica* (a hermaphrodite) weighing 150–500 g were obtained from Marinus. Animals were housed in an ~300 L aquarium containing continuously circulating, aerated artificial sea water (Instant Ocean, Aquarium Systems) at 14−16°C on a 12 h light/dark cycle and fed Romaine lettuce five times per week. For primary cultures of isolated bag cell neurons, animals were anesthetized by an injection of isotonic $MgCl_2$ (~50% body weight), the abdominal ganglion removed, and incubated for 18 h at 22°C in neutral protease (13.33 mg/ml; 165859, Roche Diagnostics) dissolved in tissue culture artificial sea water (tcASW; composition in mM: 460 NaCl, 10.4 KCl, 11 $CaCl_2$, 55 $MgCl_2$, 15 HEPES, 1 mg/ml glucose, 100 U/ml penicillin, and 0.1 mg/ml streptomycin, pH 7.8 with NaOH). The ganglion was then transferred to fresh tcASW and the bag cell neuron clusters dissected from the surrounding connective tissue. Using a fire-polished Pasteur pipette and gentle trituration, neurons were dispersed onto 35 × 10 mm polystyrene tissue culture dishes (Catalog #353001; Falcon, UltiDent) filled with 2 ml of tcASW. Cultures were maintained in tcASW in a 14°C incubator and used within 1–3 d. Salts were obtained from Fisher Scientific or Sigma-Aldrich.

Sharp-electrode current-clamp recording. Current-clamp recordings were made using an AxoClamp 2B amplifier (Molecular Devices) and the sharp-electrode, bridge-balanced method. Microelectrodes were pulled from 1.2 mm external, 0.9 mm internal diameter borosilicate glass capillaries (TW120F-4; World Precision Instruments) and had a resistance of 15–30 MΩ when filled with 2 M K-acetate plus 10 mM HEPES and 100 mM KCl, pH 7.3, with KOH. Recordings were performed in normal artificial sea water (nASW; composition according to tcASW but lacking glucose, penicillin, and streptomycin) or Na^+-free ASW (sfASW), where Na^+ was replaced with *N*-methyl-D-glucamine (NMDG). For some experiments, the extracellular Ca^{2+} concentration in the nASW external was increased to produce a high Ca^{2+} solution by equimolar replacement of $CaCl_2$ for $MgCl_2$ (16.5 mM $CaCl_2$ and 49.5 mM $MgCl_2$). All neurons used had resting potentials of −50 to −60 mV and action potentials that overshot 0 mV in response to depolarizing current injection. Current was delivered with a S88 stimulator (Grass). Voltage was filtered at 3 kHz using the Axoclamp built-in Bessel filter and sampled at 2 kHz using an IBM compatible personal computer and a Digidata 1322A analog-to-digital converter and the Clampex acquisition program of pClamp software (v10.2; Molecular Devices).

Whole-cell, voltage-clamp recording. Voltage-clamp recordings were made using an EPC-8 amplifier (HEKA Electronics) and the tight-seal, whole-cell method. Microelectrodes were pulled from 1.5 mm external, 1.2 mm internal diameter borosilicate glass capillaries (TW150F-4, World Precision Instruments) and had a resistance of 1–2 MΩ when filled with intracellular saline (see below). We found that pipettes in this size range were essential to entirely prevent the enhancement of Ca^{2+} current by post-whole-cell treatment with PMA. Higher resistance pipettes allowed for modest (~25%) increase in Ca^{2+} current after PMA post-whole-cell. For recording, pipette junction potentials were nulled, and subsequent to seal formation, pipette capacitive current were cancelled. To facilitate membrane capacitance tracking (see Capacitance tracking, below), series resistance and whole-cell capacitance were usually not compensated. However, when recording Ca^{2+} current the series resistance (2–5 MΩ) was compensated to 70–80% while the neuronal capacitance current was cancelled. Current was filtered at 1 kHz by the EPC-8 built-in Bessel filter and sampled at 2 kHz as described in *Sharp-electrode current-clamp recording*. Clampex was also used to set the holding and command potentials. Ca^{2+} current were isolated using Ca^{2+}-Cs^+-tetraethylammonium (TEA) ASW, as per tcASW, but with the NaCl and KCl replaced by TEA-Cl and CsCl, respectively, and the glucose and antibiotics omitted (composition in mM: 460 TEA-Cl, 10.4 CsCl, 55 $MgCl_2$, 11 $CaCl_2$, 15 HEPES, pH 7.8 with CsOH). In some cases, the extracellular Ca^{2+} concentration was increased to produce a high-Ca^{2+} solution by equimolar replacement of $CaCl_2$ for $MgCl_2$ (16.5 mM $CaCl_2$ and 49.5 mM $MgCl_2$). Whole-cell recordings used a Cs^+-aspartate-based intracellular saline [composition in mM: 70 CsCl, 10 HEPES, 11 glucose, 10 glutathione, 5 EGTA, 500 aspartic acid, 5 ATP (grade 2, disodium salt; A3377, Sigma-Aldrich), and 0.1 GTP (type 3, disodium salt; G8877, Sigma-Aldrich), pH 7.3 with CsOH]. To image Ca^{2+} (see Calcium imaging, below) under whole-cell voltage-clamp, the intracellular saline was supplemented with 1 mM fura-PE3 (0110; Teflabs) to dye-fill neurons via passive dialysis.

Capacitance tracking. As an indicator of secretion, membrane capacitance was tracked on-line under whole-cell voltage-clamp using the time-domain method in Clampex. Our prior work indicated that this method could consistently detect the Ca^{2+}-dependent exocytosis of ELH from bag cell neurons (Hickey et al., 2013). From a holding potential of −80 mV, pulses of 100 ms duration and 20 mV amplitude were delivered at 0.5–2 Hz. The voltage step evoked voltage-independent current responses, consisting of a fast transient component (reflecting capacitive current) followed by a steady-state component (reflecting membrane current). The change in current (ΔI) to the +20 mV step (ΔV) was calculated as the difference between the steady-state current (I_{ss}) near the end of the step and the baseline current (I_b) before the step: $\Delta I = I_{ss} - I_b$. The membrane time constant (τ) was derived by fitting a single exponential to the transient current. The charge during the transient current (Q_{tc}) was determined by integrating the area above I_{ss} for the period of the transient current. A correction factor (Q_{cf}), to account for the settling time during the step, was calculated as follows: $Q_{cf} = \Delta I \times \tau$. The total charge ($Q_t$) was then determined by: $Q_t = Q_{tc} + Q_{cf}$. The total resistance (R_t) was calculated as follows: $R_t = \Delta V/\Delta I$, whereas access resistance (R_a) was derived from: $R_a = \tau \times \Delta V/Q_t$. These were used to calculate membrane resistance (R_m) as follows: $R_m = R_t - R_a$. Finally, membrane capacitance (C_m) was determined from: $C_m = Q_t \times R_t/\Delta V \times R_m$. To increase the accuracy and improve the signal-to-noise ratio, current traces were cumulatively averaged (5–10 pulses per calculation). The −80 mV holding potential was chosen to avoid the activation of any voltage-gated Ca^{2+} channels during the 20 mV step.

For the 5 Hz, 5 or 60 s stimuli, membrane capacitance tracking was interrupted at the start of the train and restarted at the end of the stimulus. However, during the 1 Hz, 10 min train, the stimulus was interrupted every ~10 s to briefly (~1 s) apply test pulses to assay the development of exocytosis. Intermittent test pulses were not used during the 5 and 60 s stimuli because, unlike the 10 min stimulus, the former were shorter and at a faster frequency, meaning interruption of acquisition would disrupt Ca^{2+} influx and/or capacitance responses. For presentation, capacitance data were imported to Origin (v. 7.0; OriginLab) and adjacently averaged (5 points). Similar to reports in other cell types (Hsu and Jackson, 1996) a steady negative drift in membrane capacitance was often present. Therefore, for the presentation of some sample traces, the slope of the baseline drift was calculated in pClamp and subtracted from the capacitance measurements. There were no apparent differences in drift magnitude between experimental conditions.

Calcium imaging. To perform Ca^{2+} imaging, fura-PE3 was introduced either by dialysis via the whole-cell pipette during voltage-clamp recordings or by pressure injecting concentrated fura-PE3 (10 mM) with sharp-electrodes using a PMI-100 pressure microinjector (Dagan). For the latter, microelectrodes (as per Sharp-electrode current-clamp, above) had a resistance of 15–20 MΩ when the tip was filled with 10 mM fura-PE3 then backfilled with 3 M KCL. Injections required 10–20 0.2 ms pulses at 50–100 kPa to fill the neurons with an optimal amount of dye, estimated to be 50–100 μM. All neurons used subsequently for imaging showed resting potentials of −50 to −60 mV and displayed action potentials that overshot 0 mV following depolarizing current injection (0.5–1 nA, directly from the amplifier). After dye injection, neurons were allowed to equilibrate at least 30 min before recording.

All Ca^{2+} imaging was performed using a TS100-F inverted microscope (Nikon) equipped with a Nikon Plan Fluor 20× [numerical aperture (NA) = 0.5] or Plan Fluor 40× oil objective (NA = 1.3). The light source was a 75 W Xe arc lamp and a multiwavelength DeltaRAM V monochromatic illuminator (Photon Technology International) coupled to the microscope with a UV-grade liquid-light guide. Excitation wavelengths were 340 and 380 nm. The excitation illumination was controlled by a shutter, which along with the excitation wavelength, was controlled by a computer, a Photon Technology International computer interface, and EasyRatio Pro software (v1.10, Photon Technology International). To allow for continuous image acquisition during experiments, the shutter remained open. Emitted light passed through a 400 nm long-pass dichroic mirror and a 510/40 nm emission barrier filter before being detected by a Photometrics Cool SNAP HQ2 charge-coupled device camera. The ratio of the emission following 340 and 380 nm excitation (340/380) was taken to reflect free intracellular Ca^{2+} (Grynkiewicz et al., 1985), and saved for subsequent analysis. Image acquisition, emitted light sampling, and ratio calculations were performed using EasyRatio Pro.

Most Ca^{2+} measurements were acquired from a somatic region of interest at approximately the midpoint of the vertical focal plane and one-half to three-quarters of the cell diameter. Camera gain was maximized, pixel binning was set at 2, exposure time at each wavelength was fixed to ∼1 s, and images (696 × 520 pixels) were averaged eight frames per acquisition. During Ca^{2+} measurements from neurites, pixel binning was set to 4, exposure time at each wavelength was fixed to ∼1.5 s, and averaged eight frames per acquisition, for an acquisition rate of 1 ratiometric image (348 × 260 pixels) every ∼3 s. Ratiometric images used for presentation were produced from 340/380 nm images after removing the mean background signal (measured in cell-free areas) from each image.

Immunocytochemistry. Bag cell neurons colabeled with MitoTracker and anti-ELH, were prepared as described in *Animals and cell culture*, with the exception that neurons were plated onto glass coverslips (no. 1; 48366045; VWR) coated with 1 μg/ml poly-L-lysine hydrobromide, MW = 300,000 (P1534–25MG; Sigma-Aldrich) and glued with Sylgard silicone elastomer (SYLG184; World Precision Instruments) to holes drilled out of the bottom of the tissue culture dish. Before fixation, cells were treated with 500 nM (in DMSO) of the fixable dye MitoTracker Red CMXRos (M-7512; Invitrogen) for 30 min. Subsequently, the dish was drained of all fluid except for the contents of the glass-bottom well and new solutions delivered by Pasteur pipette directly onto the cells. Neurons were fixed for 25 min with 4% (w/v) paraformaldehyde (04042; Fisher Scientific) in 400 mM sucrose/nASW, pH 7.5 with NaOH. They were then permeabilized for 5 min with 0.3% (w/v) Triton X-100 (BP151; Fisher Scientific) in fix and washed twice with PBS (composition in mM: 137 NaCl, 2.7 KCl, 4.3 Na_2HPO_4, 1.5 KH_2PO_4, pH 7.0 with NaOH). Neurons were blocked for 60 min in a blocking solution of 5% (v/v) goat serum (G9023; Sigma-Aldrich) in PBS. The primary antibody, rabbit anti-ELH IgG (kindly provided by Dr N. L. Wayne, University of California, Los Angeles), was applied at 1:1000 in blocking solution. Neurons were incubated in the dark for 1 h and subsequently washed four times with PBS. The secondary antibody, goat anti-rabbit IgG conjugated to AlexaFluor 488 (A-11008; Invitrogen) was applied at 1:200 in blocking solution and incubated in the dark for 2 h. Neurons were then washed four times with PBS, the wells filled with mounting solution [26% w/v glycerol (BP2291; Fisher Scientific), 11% w/v Mowiol 4-88 (17951; Polysciences), and 110 mM TRIS, pH 8.5], and covered with a glass coverslip. Stained neurons were imaged using the Nikon TS100-F microscope equipped with a Nikon Plan Fluor 20× oil-immersion (NA = 0.75) or Nikon Plan Fluor 100× oil-immersion objective (NA = 1.3). Neurons were excited with a 50 W Hg lamp and a 480/15 nm bandpass filter. Fluorescence was emitted to the eyepiece or camera through a 505 nm dichroic mirror and a 520 nm barrier filter. Images (1392 × 1040 pixels) were acquired at the neurite focal plane using a Pixelfly USB camera (PCO-TECH, Photon Technology International) and the Micro-Manager 1.4.5 plugin for ImageJ 1.43 with 100–2000 ms exposure times.

Reagents and drug application. Solution exchanges were accomplished by manual perfusion using a calibrated transfer pipette to first exchange the bath (tissue culture dish) solution. In most cases where a drug was applied, a small volume (∼4 μl) of concentrated stock solution was mixed with a larger volume of saline (∼100 μl) that was initially removed from the bath, and this mixture was then pipetted back into the bath. Tetrodotoxin citrate (TTX; T-550; Alomone Labs) was dissolved in water as a vehicle. Phorbol 12-myristate 13 acetate (PMA;P8139; Sigma-Aldrich), latrunculin B (Lat B; L5288, Sigma-Aldrich), H-7 (I7016; Sigma-Aldrich), carbonyl cyanide 4-(trifluoromethoxy) phenylhydrazone (FCCP; 21857; Sigma-Aldrich) all required dimethyl sulfoxide (DMSO; BP231, Fisher Scientific) as a vehicle. The maximal final concentration of DMSO was 0.05–0.5% (v/v) which, in control experiments as well as prior work from our laboratory, had no effect on membrane potential, various macroscopic or single channel current, resting intracellular Ca^{2+}, or Ca^{2+} transients evoked by action potentials (Lupinsky and Magoski, 2006; Hung and Magoski, 2007; Gardam et al., 2008; Geiger and Magoski, 2008; Tam et al., 2009, 2011; Hickey et al., 2013).

Data analysis and statistics. To quantify Ca^{2+} current magnitude, the peak current of each trace was measured in Clampfit, a program of pClamp, between cursors set at the start and end of the trace, and then divided by whole-cell capacitance. Activation curves were produced by dividing the current elicited at each voltage step by the maximum current elicited during the protocol. This was averaged across cells at a given step voltage, plotted against that voltage, and fit with a Boltzmann equation in Origin. Activation and inactivation time constants were acquired by fitting monoexponential decay functions to the activation and inactivation components of the Ca^{2+} current. The activation time period was defined as the time from the start of the inward current (after the small capacitance current) to the peak inward current. Conversely, the inactivation period was fitted to the range of time from the peak Ca^{2+} current to the last measurable point before the end of the depolarizing test pulse and the start of the capacitance artifact. Peak action potential height was measured in a similar fashion as Ca^{2+} current. To produce group data, the average height of 10 serially evoked action potentials before and after 5–10 min of PMA were compared. To quantify membrane capacitance, Clampfit was used to compare the average value during a steady-state baseline of 30 s to 1 min, with either the peak response following a train of depolarizing stimuli or the average value from a region that had reached peak for 5–30 s. Average values were determined by eye or by setting cursors on either side of the range of interest and calculating the mean of those data points. Change was expressed as a percentage change of the new capacitance over the baseline capacitance. Analysis for Ca^{2+} imaging data acquired with ImageMaster Pro was performed in Origin. The steady-state value of the baseline 340/380 ratio was compared with the ratio from regions that had reached a peak (340/380 peak − prestimulus baseline 340/380). Averages of the baseline and peak regions were resolved by eye or with adjacent-averaging (5 points). For presentation, traces were selected that best represented the mean peak Ca^{2+} or capacitance responses and then aligned at the prestimulus baselines for each condition regardless of their absolute baseline value.

Statistics were performed using Instat (v. 3.0; GraphPad Software). Summary data are presented as the mean ± SEM. The Kolmogorov–Smirnov method was used to test datasets for normality. If the data were normal, Student's paired or unpaired *t* test was used to test for differences between two means, while a standard one-way ANOVA with a Tukey multiple-comparisons test was used to test for differences between multiple means. If the data were not normally distributed, a Mann–Whitney *U* test was used for two means, whereas a Kruskal–Wallis (KW) ANOVA with Dunn's multiple-comparisons test was used for multiple means. Data were considered significantly different at $p < 0.05$.

Results

Activation of PKC increases voltage-gated Ca^{2+} current and potentiates exocytosis to an afterdischarge-like stimulus

The influence of PKC on ion channel function can be observed in cultured bag cell neurons following microinjection of PKC itself or incubation with the phorbol ester, PMA, which directly activates PKC (Castagna et al., 1982; DeRiemer et al., 1985; Conn et al., 1989b; Sossin et al., 1993). To confirm this, we evoked action potentials from cultured bag cell neurons using sharp-electrode current-clamp, before and after bath application of 100 nM PMA ($n = 4$). By ~5 min of PMA, action potential height significantly increased for the duration of the recording (Fig. 1*A*, left and middle). Prior work indicates that PMA enhances action potentials by inducing the rapid, PKC-dependent recruitment of Apl Ca_v2 (Strong et al., 1987; Conn et al., 1989b; Zhang et al., 2008). The upstroke of the bag cell neuron action potential can also contain a Na^+ component (Acosta-Urquidi and Dudek, 1980; Fieber, 1995). To ensure that changes to spike height are mediated by Ca^{2+} current, we assessed the ability of PMA to enhance spike height in the absence of extracellular Na^+ (with $NMDG^+$ as a substitute). Under these conditions, PMA still augmented action potential height to an extent that reached significance ($n = 5$; Fig. 1*A*, right).

Next, we confirmed the effect of PMA on Apl Ca_v2 insertion by measuring Ca^{2+} current isolated under whole-cell voltage-clamp with a TEA- and Cs^+-based external solution and a Cs^+-based intracellular solution. Unless stated otherwise, all subsequent whole-cell voltage-clamp recordings were made using these solutions. Compared with control cells, Ca^{2+} current caused by a series of 200 ms step depolarizations from −60 to +60 mV, was substantially larger in neurons treated with 100 nM PMA for 15 min before establishing whole-cell configuration (Fig. 1*B*).

The bag cell neurons secrete ELH and other related peptides from both the soma and the primary neurites, the correlates of the neurosecretory endings *in vivo* (Frazier et al., 1967; Kaczmarek et al., 1979; Hatcher et al., 2005, Hatcher and Sweedler, 2008; Hickey et al., 2013). Consistent with a possible role in facilitating hormone output, Apl Ca_v2 α-1 subunits appear in both regions after engaging PKC (Zhang et al., 2008). We assessed the impact of Apl Ca_v2 insertion on stimulus-evoked Ca^{2+} entry in the neurites and soma by ratiometrically imaging fura-PE3-injected bag cell neurons current-clamped at −60 mV with somatic sharp-electrode recording. Strong current pulses (15 ms, ~6–8 nA) were used to ensure that action potentials were consistently elicited during train stimuli. To avoid dye saturation, a short 5 Hz, 5 s train of depolarizing current pulses was delivered. Before PMA, the train produced a transient Ca^{2+} rise in the primary neurites (Fig. 1*C*). Within 5–10 min of exposure to 100 nM PMA, there was an ~30% enhancement of Ca^{2+} influx in response to the same train stimulus ($n = 12$; Fig. 1*C*). A similar outcome was also confirmed in the soma ($n = 5$; Fig. 1*C*, right).

We next assessed whether PKC could alter secretion from bag cell neurons by tracking membrane capacitance under whole-cell voltage-clamp: a widely used method for assaying plasma membrane area changes caused by vesicle fusion (Neher and Marty, 1982). To monitor exocytosis in response to physiological-like patterns, neurons were stimulated with a 5 Hz, 60 s train of 75 ms depolarizing steps from −80 to 0 mV, which mimics the fast-phase of the afterdischarge (Kupfermann and Kandel, 1970; Kaczmarek et al., 1982). Applying this stimulus to control neurons (treated with DMSO, the vehicle; $n = 13$) elicited Ca^{2+} current and an elevation in membrane capacitance that decayed to baseline in 5–10 min (Fig. 1*D*, left). Previous work by our laboratory and others has demonstrated that this capacitance response reflects the exocytosis of vesicles containing ELH and related peptides (Hatcher et al., 2005; Hickey et al., 2013). Neurons treated with 100 nM PMA for 15 min before establishing whole-cell configuration ($n = 10$) showed larger Ca^{2+} current to the 60 s train and a capacitance rise that was twice the magnitude of control (Fig. 1*D*, left and right, *E*).

Whole-cell dialysis disrupts Apl Ca_v2 recruitment

Based on structure, Apl Ca_v1 and Apl Ca_v2 belong to the Ca_v1 and Ca_v2 voltage-gated Ca^{2+} channel α-1 subunit families, respectively (White and Kaczmarek, 1997). Unlike their vertebrate counterparts, macroscopic current mediated by the Apl Ca_v1 and Apl Ca_v2 α-1 subunits have similar kinetics, voltage dependence, and pharmacological sensitivity (McCleskey et al., 1987; Strong et al., 1987; Fieber, 1995). Nevertheless, these channels can be distinguishing based on their sensitivity to whole-cell recording conditions. Performing whole-cell dialysis before, but not after engaging PKC with PMA, prevents the detection of Apl Ca_v2 Ca^{2+} current (DeRiemer et al., 1985; Strong et al., 1987), which may be expected given that Apl Ca_v2 transitions from an intracellular pool to a membrane ion channel. In contrast, whole-cell recording does not disrupt other PMA-induced forms of ion channel modulation in the bag cell neurons, including Ca^{2+}-activated K^+ and nonselective cation channels (Zhang et al., 2002; Tam et al., 2011). Despite early reports, a thorough analysis of this effect on macroscopic Ca^{2+} current has yet to be published; therefore, we used step depolarizations to systematically assay the current–voltage relationship of Ca^{2+} current when PKC is triggered before or after whole-cell dialysis. The chronology of drug treatments with respect to the establishment of whole-cell recordings is shown in Figure 2*A*. Neurons in DMSO ($n = 20$), which lack PKC activity and use only Apl Ca_v1, presented moderately sized Ca^{2+} current (Fig. 2*A*, top, *B*, top, *C*). To engage PKC and Apl Ca_v2, other neurons were treated with 100 nM PMA for 15 min before whole-cell breakthrough ($n = 21$). As in Figure 1, the resulting Ca^{2+} current was much larger than control (Fig. 2*A*, middle, *B*, middle, *C*). In contrast, triggering PKC in the absence of Apl Ca_v2 mobilization, by applying PMA for 15 min subsequent to obtaining whole-cell configuration ($n = 9$), resulted in Ca^{2+} current that was essentially identical to control (Fig. 2*A*, bottom, *B*, bottom, *C*). We also elucidated the impact of PKC activation post-whole-cell by monitoring the change in peak Ca^{2+} current elicited by 0.03 Hz, 75 ms pulses to 0 mV from −60 mV. Unlike the influence of PMA on action potential height and Ca^{2+} influx measured with sharp-electrode, even several minutes after introducing PMA ($n = 5$), the Ca^{2+} current remained constant under whole-cell conditions (Fig. 2*D*).

Prior work from others and our laboratory indicates that, aside from a general enhancement of Ca^{2+} current, there is little apparent change in the voltage dependence or kinetics of macroscopic Ca^{2+} current after Apl Ca_v2 is engaged. Using the Ca^{2+} current presented in Figures 1*C* and 2*C*, we assessed the voltage dependence of activation for cells treated with either DMSO, PMA pre-whole-cell, or PMA post-whole-cell. An I/I_{max} plot was created, where Ca^{2+} current for each condition was normalized to the largest current evoked during the pulse protocol (typically 0 or +10 mV) and plotted against test pulse voltage. After fitting a Boltzmann function to each curve, it was apparent that PMA pre-whole-cell and PMA post-whole-cell were slightly left-shifted

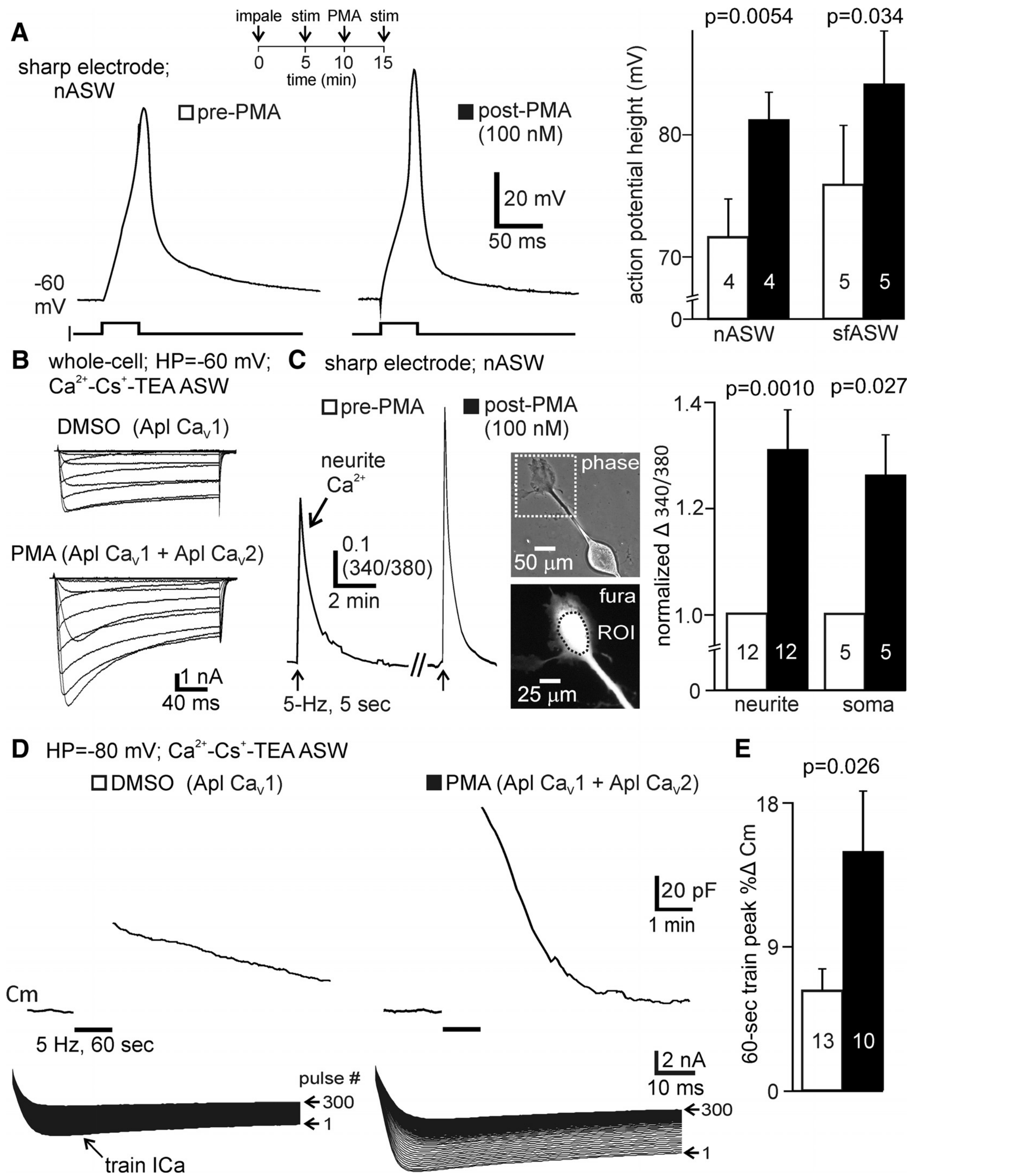

Figure 1. PMA-induced membrane insertion of Apl Ca_v2 channels is associated with an enhancement of exocytosis in cultured bag cell neurons. ***A***, Left, Midde, Action potentials from a cultured bag cell neuron bathed in nASW stimulated under sharp-electrode current-clamp increase in height within ~5 min of 100 nM PMA addition. Right, Group data show that PMA significantly increases peak action potential height when the extracellular solution is either Na^+-containing (nASW) or Na^+-free (sfASW; NMDG ion substituted; paired Student's *t* test for both). Data represent the mean ± SEM with the number of neurons (*n*) indicated within bar graphs. ***B***, Whole-cell voltage-clamp recordings of voltage-gated Ca^{2+} current evoked from bag cell neurons by 200 ms square pulses from a holding potential (HP) of −60 to +60 mV in 10 mV increments using Ca^{2+}-Cs^+-TEA-based external and Cs^+-based intracellular solutions. Compared with a neuron exposed to DMSO (top), a second neuron treated with 100 nM PMA for ~15 min (bottom), before establishing whole-cell configuration, shows elevated Ca^{2+} current due to Apl Ca_v2 recruitment supplementing the basal Apl Ca_v1 current. ***C***, Left, Ca^{2+} influx in a distal neurite measured by the change in the emission intensity with 340/380 excitation following action potentials initiated from the soma by a 5 Hz, 5 s train of depolarizing current pulses under sharp-electrode current-clamp. In control, the train of action potentials produces a moderate rise in neurite Ca^{2+}. After engaging Apl Ca_v2 channels with ~5 min of PMA, the same stimulus causes a substantially larger peak Ca^{2+} influx. Middle, Phase (top) and fluorescent (bottom) images of a fura-PE3-injected cultured bag cell neuron and the region-of-interest (ROI) in the distal neurite used for quantitation. Right, Summary data showing peak 340/380 rise during train stimuli normalized to the response in the pre-PMA condition. In both regions, the peak 340/380 ratio during the 5 s train is significantly increased by PMA (paired Student's *t* test for both). ***D***, Top, To monitor exocytosis, bag cell neurons are whole-cell voltage-clamped at −80 mV while membrane capacitance is tracked before and after a 5 Hz, 60 s train of 75 ms steps from −80 to 0 mV. The break in the capacitance record corresponds to the train application. Left, In control (DMSO) neurons, stimulation opens only basal Apl Ca_v1 current (bottom) and evokes a moderate rise in membrane capacitance. Right, Neurons in which Apl Ca_v2 current (bottom) is recruited by ~15 min of PMA pre-whole-cell show a much larger capacitance change to the 60 s train. ***E***, The mean peak percentage change in capacitance to the train-stimulus is significantly larger following PMA pre-whole-cell versus DMSO-treated cells (Mann–Whitney *U* test).

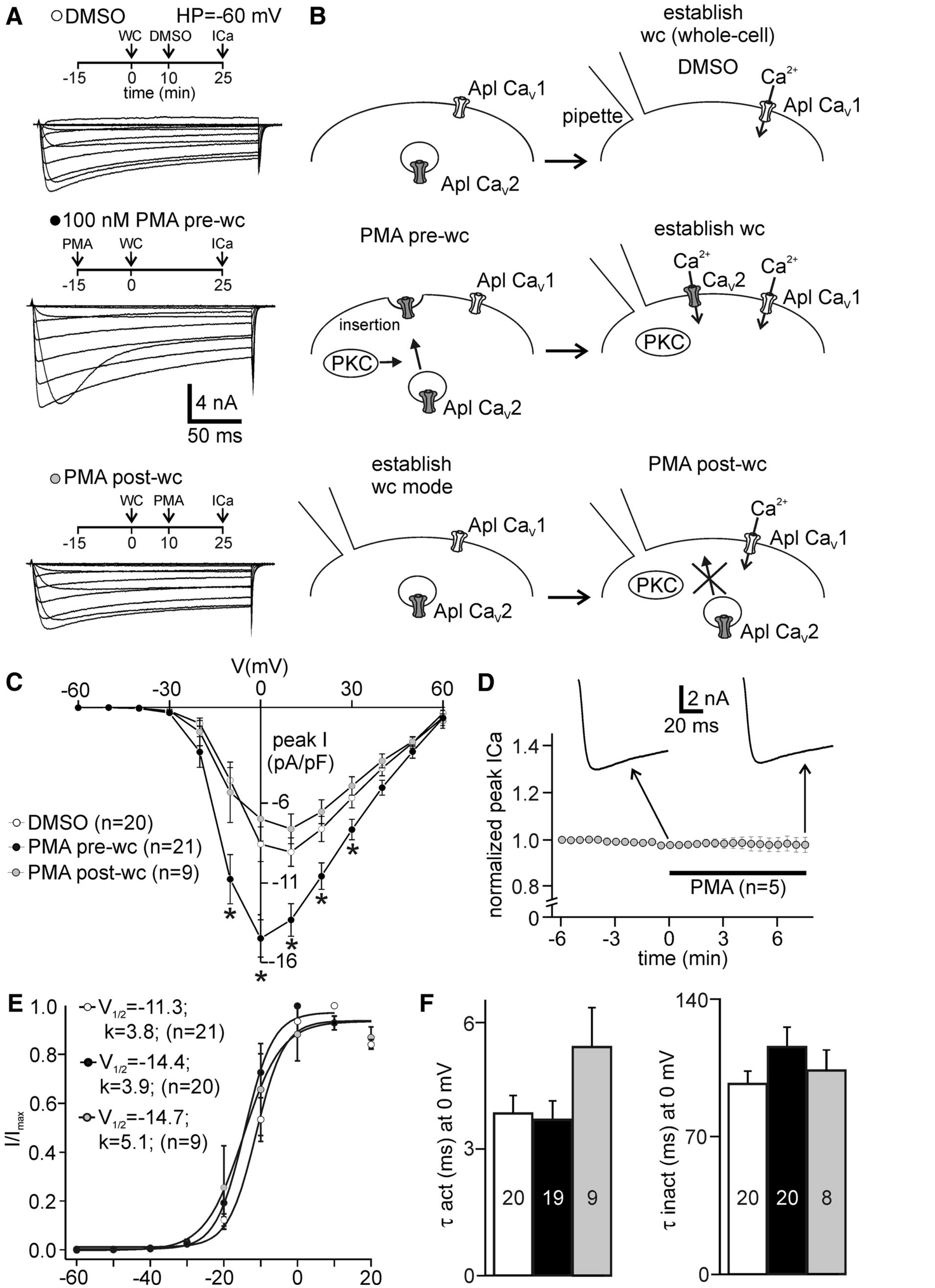

Figure 2. PMA-induced enhancement of voltage-gated Ca^{2+} current is disrupted by prior establishment of whole-cell configuration. ***A***, Whole-cell voltage-clamp recordings of Ca^{2+} current evoked by 200 ms square pulses from −60 to +60 mV in 10 mV increments. Compared with a neuron exposed to DMSO (top), a different neuron given 100 nM PMA for ∼15 min pre-whole-cell (pre-wc; middle) shows a large enhancement in current due to the insertion of Apl Ca$_v$2. In a third neuron, activating PKC with PMA post-whole-cell (post-wc; lower) does not engage Apl Ca$_v$2, as shown by similar-sized current to DMSO. ***B***, Conceptual model for the disruption of Apl Ca$_v$2 recruitment by intracellular dialysis (based on DeRiemer et al., 1985; Strong et al., 1987). Top, In untreated neurons, only the basal Apl Ca$_v$1 channel is in the membrane when whole-cell configuration is established. Middle, Delivering PMA before achieving whole-cell (*Figure legend continues.*)

in voltage dependence of activation, as indicated by the $V_{1/2}$ of activation (DMSO $V_{1/2}$: −11.3 mV; PMA pre-whole-cell: −14.4 mV; PMA post-whole-cell: −14.7 mV; Fig. 2*E*). The *k* values indicated a subtle decrease in the voltage sensitivity in cells treated with PMA post-whole-cell ($k = 5.1$) but not PMA pre-whole-cell ($k = 3.9$) compared with DMSO ($k = 3.8$). Ca^{2+} current kinetics at 0 mV were also assessed by fitting the activation and inactivation components with mono-exponential functions. The time constants acquired from each fit showed that the activation or inactivation kinetics of current were not significantly different between cells treated with either DMSO, PMA-pre-whole-cell, or PMA post-whole-cell (Fig. 2*F*).

Disrupting Apl Ca_v2 recruitment with whole-cell dialysis prevents the PMA-dependent facilitation of train-evoked exocytosis

Because Ca^{2+} influx is required for secretion, we next evaluated the impact of disrupting Apl Ca_v2 insertion on somatic Ca^{2+} entry by ratiometrically recording from fura-PE3-loaded bag cell neurons under whole-cell voltage-clamp. Ca^{2+} entry was initiated by delivering a 5 Hz, 5 s train of 75 ms steps to 0 mV from −80 mV. In DMSO ($n = 13$), opening Apl Ca_v1 channels with this train produced a transient rise in intracellular Ca^{2+} followed by recovery to baseline (Fig. 3*A*, left, *B*). After engaging Apl Ca_v2 with 100 nM PMA for 15 min pre-whole-cell ($n = 9$), the 5 s train produced a more prominent Ca^{2+} rise than control (Fig. 3*A*, middle, *B*). Conversely, neurons treated with PMA for 15 min post-whole-cell ($n = 13$) presented Ca^{2+} changes similar to DMSO (Fig. 3*A*, right, *B*). Interestingly, cells incubated in PMA pre-whole-cell had a prestimulus baseline 340/380 ratio (0.30 ± 0.027) that was significantly larger than in PMA post-whole-cell (0.22 ± 0.005) but not DMSO control (0.23 ± 0.007; $H = 8.97$, df = 2, $p < 0.02$, KW one-way ANOVA; DMSO vs PMA pre-whole-cell, $p > 0.05$; DMSO vs PMA post-whole-cell, $p > 0.05$; PMA pre-whole-cell vs PMA post-whole-cell $p < 0.01$; Dunn's multiple-comparisons test). This may suggest that the basal Ca^{2+} entry of bag cell neurons (Geiger et al., 2009) was modestly greater in PMA pre-whole-cell because of inserted Apl Ca_v2 channels. To confirm the involvement of PKC in the PMA-dependent changes in train-evoked Ca^{2+} signals, we repeated these experiments in the presence of H-7, a selective inhibitor of PKC in bag cell neurons (Conn et al., 1989a). Neurons exposed to 100 μM H-7 for 15 min before PMA pre-whole-cell ($n = 10$) showed moderate train Ca^{2+} responses, similar to those measured from cells administered H-7 alone ($n = 11$) or H-7 plus PMA post-whole-cell ($n = 9$; Fig. 3*C*,*D*).

The influence of PMA on processes independent of Apl Ca_v2 enlistment was also determined by monitoring basal Ca^{2+} during the introduction of PMA post-whole-cell. PMA had no apparent effect on resting Ca^{2+} for the ~10 min recording period (Δ340/380 at 5 min post-PMA: 0.0038 ± 0.00381, $n = 7$). Only occasionally (2/7 cells) was there a slow and small elevation in intracellular Ca^{2+} (~0.01 and ~0.02 Δ340/380). Furthermore, measurement of membrane capacitance during PMA post-whole-cell showed no detectable change ($n = 12$). It may also be possible that, with the absence of extracellular Na^+, the enhancement of train Ca^{2+} by PMA is mediated by Ca^{2+} entry via Na^+ channels. Thus, we examined the sensitivity of train-evoked Ca^{2+} responses to Na^+ channel blockade with 1 μM TTX, a concentration that entirely occludes bag cell neuron Na^+ current (Fieber, 1995), following PMA-elicited potentiation of Ca^{2+} entry. A 5 min application of TTX had no significant impact on the peak Ca^{2+} responses during the 5 Hz, 5 s train compared with PMA pre-whole-cell alone (Δ340/380 PMA pre-whole-cell: 0.070 ± 0.023, $n = 8$; Δ340/380 PMA pre-whole-cell + TTX = 0.072 ± 0.038, $n = 8$; $p = 0.72$; Mann–Whitney *U* test).

Although the sensitivity of Apl Ca_v2 to whole-cell dialysis could be considered an experimental barrier, we used it as a tool for the present study. Aside from enhancing Ca^{2+} influx, it is feasible that PKC promotes peptide secretion by changing the readily releasable pool, peptide vesicle trafficking, or Ca^{2+}-sensitivity of secretion (Gillis et al., 1996; Yang et al., 2002; Zhu et al., 2002). As mentioned, in the bag cell neurons the activity of PKC itself is not altered by recording conditions (Zhang et al., 2002; Tam et al., 2011). Thus, whole-cell dialysis is ideal for examining these possibilities, as it selectively prevents Apl Ca_v2 recruitment while allowing PKC to act on other targets. To examine whether PKC facilitates peptide secretion, independent of Apl Ca_v2, capacitance responses to a 5 Hz, 60 s train were measured in neurons given 100 nM PMA before or after establishing whole-cell mode. As previously demonstrated, neurons treated with 100 nM PMA pre-whole-cell ($n = 23$) present a substantial augmentation of capacitance responses to the 60 s train relative to control cells ($n = 19$; Fig. 3*E*, left vs middle). Conversely, cells in which PKC was engaged in the absence of Apl Ca_v2 mobilization (PMA post-whole-cell; $n = 18$) showed capacitance changes that were indistinguishable from control conditions (Fig. 3*E*, left vs right). This was reflected in the summary data, which showed that PMA pre-whole-cell, but not post-whole-cell, significantly increased the percentage change in membrane capacitance to the 60 s train relative to control (Fig. 3*F*).

The facilitation of train-evoked exocytosis by Apl Ca_v2 recruitment relies on the actin cytoskeleton

The dynamic rearrangement of the actin cytoskeleton by protein kinases is known to modulate secretion, typically by changing the availability of vesicles for release (Malacombe et al., 2006). Because the rapid insertion of ion channels and transporters into the plasma membrane is also mediated by interactions with the actin cytoskeleton, a similar mechanism may be at work for Ca^{2+} channels (Tong et al., 2001; Gu et al., 2010). PKC activation causes Apl Ca_v2 to associate with actin and insert into the membrane through a process that requires actin polymerization (Zhang et al., 2008). We confirmed this by measuring the impact

←

(*Figure legend continued.*) allows for the measurement of Apl Ca_v2 current, as insertion has previously occurred. Bottom, Applying PMA to neurons after whole-cell mode is achieved, activates PKC, but is unable to marshal Apl Ca_v2 channels. ***C***, The summary current–voltage relationship of peak Ca^{2+} current density from neurons exposed to PMA post-whole-cell is not significantly different from control, but is significantly smaller than PMA pre-whole-cell ($p < 0.05$, KW one-way ANOVA; *$p < 0.05$, Dunn's multiple-comparisons test for −10, 0, 10, 30 mV; $p < 0.05$, one-way ANOVA; *$p < 0.05$ Tukey–Kramer multiple-comparisons test for 20 mV). ***D***, Plot of peak Ca^{2+} current elicited by 0.03 Hz, 75 ms pulses from −60 to 0 mV, normalized to the first current, during addition of PMA post-whole-cell. There is no significant difference between 0 and 7.5 min (insets) after PMA ($p = 0.649$, paired Student's *t* test). ***E***, Activation curve for Ca^{2+} current presented in ***C***. Current is normalized to maximum current, plotted against test pulse voltage, and then fit with a Boltzmann function. As indicated by the $V_{1/2}$ values, compared with DMSO control, there is a slight leftward shift in activation for cells treated with PMA pre-whole-cell and PMA post-whole-cell. The *k* values also suggest a small change in voltage-sensitivity for PMA post-whole-cell between the conditions. ***F***, Summary graphs of activation (τ_{act}) and inactivation (τ_{inact}) time constants for Ca^{2+} current at 0 mV from the neurons presented in ***C***. There is no significant difference in either the activation (left; $H = 4.6$, df = 2, $p > 0.05$, KW one-way ANOVA) or inactivation (right; $F_{(2,45)} = 4.8$, $p > 0.05$, one-way ANOVA) between neurons exposed to DMSO, PMA pre-whole-cell, or PMA post-whole-cell. The discrepancy in *n* values between this panel and ***C***, ***E*** is due to the exclusion of a small number of neurons that present currents poorly fit by the exponential functions.

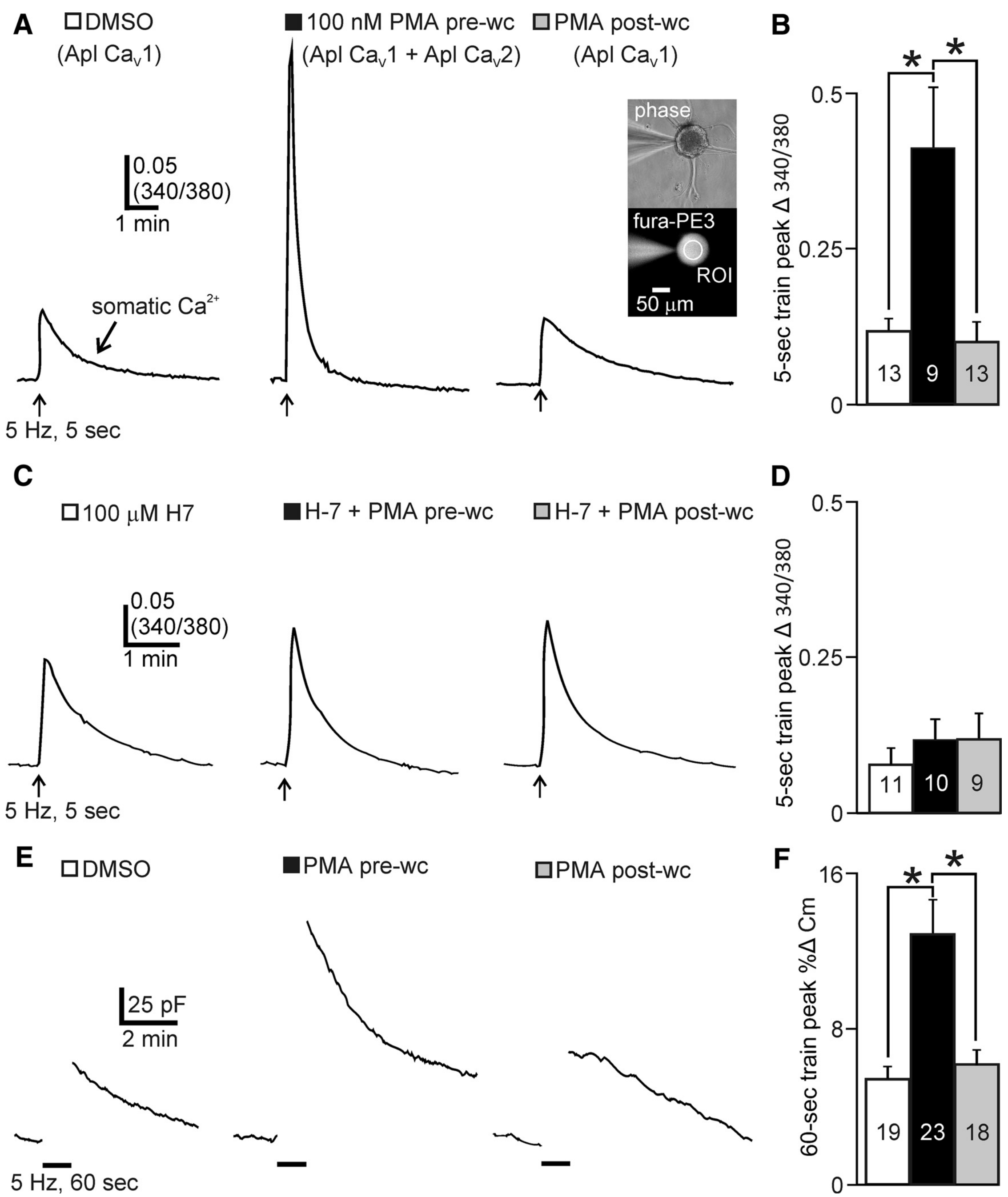

Figure 3. Disrupting the PKC-dependent Apl Ca_v2 recruitment by prior whole-cell establishment prevents PMA from facilitating secretion to train stimuli. ***A***, Inset, Phase (top) and fluorescent (bottom) images of a neuron filled with fura-PE3 and the somatic ROI used for quantification. Left, In control, a 5 Hz, 5 s train of 75 ms pulses from −80 to 0 mV produces a moderate rise in somatic Ca^{2+}. Middle, After engaging Apl Ca_v2 channels with ~15 min 100 nM PMA pre-whole-cell, the 5 s train evokes a more prominent Ca^{2+} rise. Right, Conversely, treating neurons with ~15 min of PMA post-whole-cell does not enhance Ca^{2+} influx. ***B***, PMA pre-whole-cell, but not PMA post-whole-cell, significantly increases the peak change in the 340/380 ratio during the 5 s train relative to DMSO ($H = 11.5$, df = 2, $p < 0.004$, KW one-way ANOVA; *$p < 0.05$, Dunn's multiple-comparisons test). ***C***, Intracellular Ca^{2+} measurements during a 5 s train in neurons provided with 100 µM of the PKC inhibitor, H-7, for 15 min before either DMSO (left), PMA pre-whole-cell (middle), or PMA post-whole-cell (right). After H-7, neurons administered PMA pre-whole-cell show similar Ca^{2+} responses as cells given DMSO + H-7 or PMA pre-whole-cell + H-7. ***D***, With prior H-7 exposure, PMA pre-whole-cell application does not significantly alter the peak change in the 340/380 ratio compared with H-7 or H-7 + PMA pre-whole-cell alone ($H = 1.37$, df = 2, $p > 0.05$, KW one-way ANOVA). ***E***, Capacitance tracking under voltage-clamp at −80 mV before and after a 5 Hz, 60 s train of 75 ms pulses from −80 to 0 mV, from three different neurons provided ~15 min of DMSO (left), PMA pre-whole-cell (middle), or PMA post-whole-cell (right). Unlike neurons treated with PMA pre-whole-cell, activating PKC post-whole-cell fails to strengthen the capacitance response compared with control. ***F***, Neurons in PMA pre-whole-cell present a significantly larger percentage change in capacitance to the 60 s train than to DMSO or PMA post-whole-cell ($H = 12.8$, df = 2, $p < 0.002$, KW one-way ANOVA; *$p < 0.05$, Dunn's multiple-comparisons test).

of Lat B on the enhancement of Ca^{2+} entry by PMA. This toxin binds to actin monomers and makes them unavailable for assembly into new filaments (Morton et al., 2000; Zhang et al., 2008). Neurons were given 10 µM Lat B for 60 min before 100 nM PMA for 15 min pre-whole-cell. Compared with neurons only exposed to PMA pre-whole-cell ($n = 11$), Lat B plus PMA ($n = 10$) resulted in a significantly smaller peak Ca^{2+} influx during the 5 Hz, 5 s train (Fig. 4*A*,*B*). However, in neurons not administered PMA, 60 min of Lat B did not alter the peak Ca^{2+} rise prompted by Apl Ca_v1 during the 5 s train (DMSO Δ340/380: 0.139 ± 0.068,

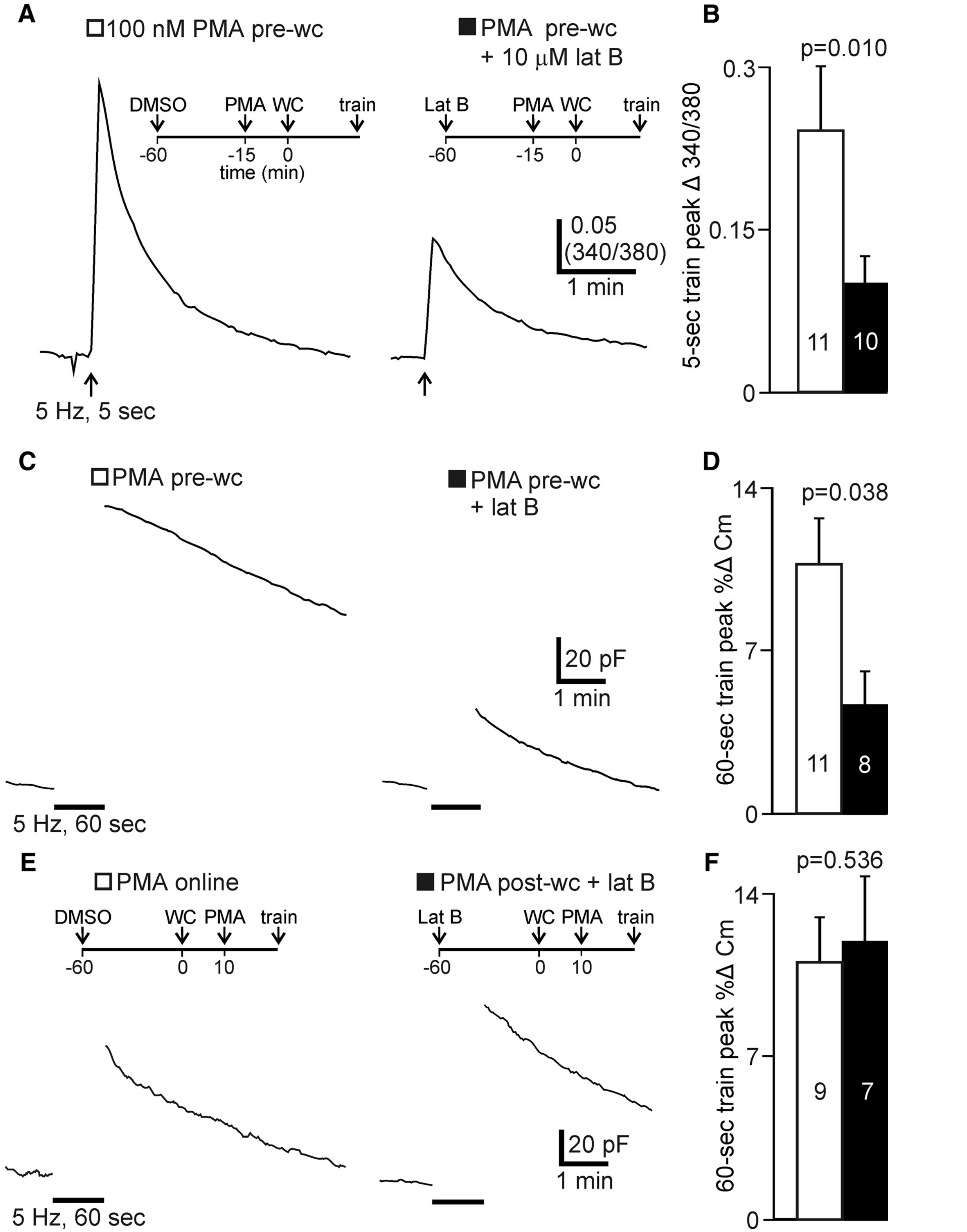

Figure 4. Inhibiting actin polymerization with Lat B prevents the PMA-dependent facilitation of train-evoked Ca^{2+} influx and exocytosis. ***A***, Neurons provided 100 nM PMA pre-whole-cell for ∼15 min show a large rise in intracellular Ca^{2+} during a 5 Hz, 5 s train of 75 ms pulses from −80 to 0 mV, which is lessened in cells bathed for 60 min in 10 μM Lat B before PMA. ***B***, Lat B before PMA pre-whole-cell significantly reduces the response to the 5 s train versus cells provided PMA pre-whole-cell alone (unpaired Mann–Whitney *U* test). ***C***, Left, Delivery of a 5 Hz, 60 s train of 75 ms pulses from −80 to 0 mV following PMA pre-whole-cell elicits a large capacitance response. Right, A neuron incubated in Lat B for 60 min before ∼15 min PMA pre-whole-cell presents a modest capacitance response. ***D***, The percentage change in the 60 s train-induced capacitance response after PMA pre-whole-cell is significantly reduced by prior introduction of Lat B (unpaired one-tailed Mann–Whitney *U* test). ***E***, Left, Capacitance response to the 60 s train from a neuron provided PMA-post-whole-cell. Right, 60 min treatment with Lat B before delivering PMA post-whole-cell does not impact the capacitance response relative to control. ***F***, Compared with cells incubated in PMA post-whole-cell alone, giving Lat B first fails to significantly alter the peak capacitance rise to the 60 s train (unpaired Mann–Whitney *U* test).

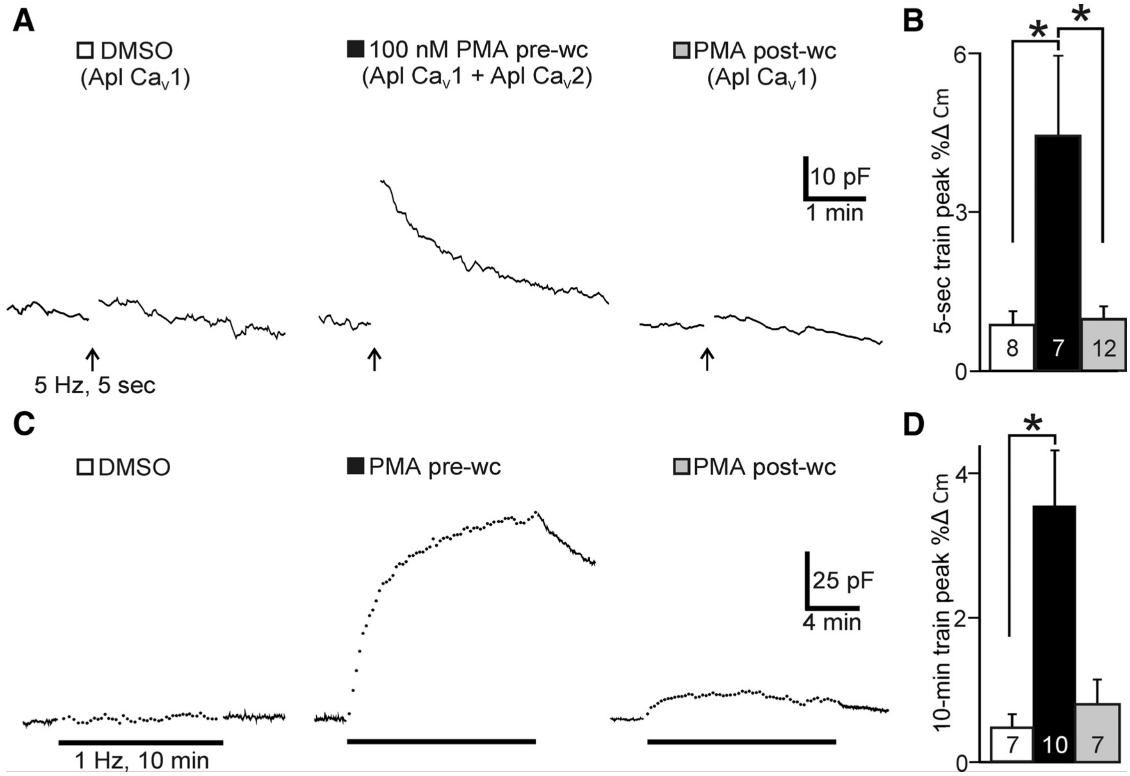

Figure 5. Recruiting Apl Ca_v2 reduces the duration and frequency of stimulation required to initiate detectable exocytosis. ***A***, Left, Applying a brief train (5 Hz, 5 s, 75 ms steps from −80 to 0 mV) produces little-to-no change in capacitance. Middle, After ~15 min incubation in 100 nM PMA pre-whole-cell to recruit Apl Ca_v2, the same train evokes a robust elevation in capacitance. Right, Delivering the 5 s train to neurons treated for ~15 min with PMA post-whole-cell, to activate PKC in the absence of Apl Ca_v2 engagement, does not increase the capacitance response. ***B***, Relative to control, the mean peak percentage change in capacitance following the 5 s train is significantly larger after PMA pre-whole-cell, but not PMA post-whole-cell ($H = 8$, df = 2, $p < 0.02$, KW one-way ANOVA; $^*p < 0.05$, Dunn's multiple-comparisons test). ***C***, Left, In DMSO, triggering Apl Ca_v1 current with a 1 Hz, 10 min train of 75 ms steps from −80 to 0 mV, to mimic the slow phase of the afterdischarge, causes essentially no capacitance change. The dotted line reflects the stimulus being interrupted every 10 s to monitor capacitance. Middle, After application of PMA pre-whole-cell to recruit Apl Ca_v2, the same 10 min train prompts a rise in capacitance which plateaus by the end of the stimulus. Right, Activating PKC in the absence of Apl Ca_v2 (PMA post-whole-cell) results in a much smaller capacitance rise. ***D***, Compared with control, the mean peak percentage change in membrane capacitance during the 10 min train is significantly larger in cells treated with PMA pre-whole-cell but not post-whole-cell ($H = 8.1$, df = 2, $p < 0.02$, KW one-way ANOVA; $^*p < 0.05$, Dunn's multiple-comparisons test).

$n = 8$; Lat B Δ 340/380: 0.116 ± 0.049, $n = 6$; $p = 0.75$, Mann–Whitney *U* test).

Having established a role for actin in Ca^{2+} influx potentiation, we next explored the impact of Lat B on peptide secretion with capacitance tracking. Compared with neurons given PMA pre-whole-cell alone ($n = 11$), incubation with Lat B ($n = 8$) for 60 min before PMA pre-whole-cell substantially reduced capacitance responses to the 5 Hz, 60 s train (Fig. 4*C*, 5*D*). In contrast, disrupting the actin cytoskeleton with Lat B in the absence of PKC had no measurable effect on the capacitance changes evoked by the train (DMSO $\%\Delta C_m$: 5.12 ± 1.2, $n = 11$; Lat B $\%\Delta C_m$: 5.62 ± 1.5, $n = 9$; $p = 0.79$, Student's *t* test). It is also possible that Lat B reduces secretion in PMA-treated neurons by altering other kinase-dependent processes not involved with Apl Ca_v2, but requiring actin polymerization. Hence, the impact of Lat B on secretion was examined in neurons subjected to PMA post-whole-cell to activate PKC in the absence of channel insertion. Applying a 60 s train to neurons exposed to Lat B for 60 min before breakthrough, and followed by 15 min of PMA post-whole-cell ($n = 7$), produced capacitance responses nearly identical to cells administered only PMA post-whole-cell ($n = 9$; Fig. 4*E*,*F*).

The recruitment of Apl Ca_v2 reduces the duration and frequency of stimulation necessary for triggering measurable exocytosis

The onset of neuropeptide secretion often requires a threshold level of Ca^{2+} entry that is obtained through either high-frequency or prolonged firing (Peng and Zucker, 1993; Soldo et al., 2004; Hickey et al., 2013). This is attributed to either the distance between vesicles and Ca^{2+} channels, a low-affinity Ca^{2+} receptor, or multiple Ca^{2+}-dependent priming steps (Thomas et al., 1993; Neher, 1998). As PKC enhances the Ca^{2+} current per action potential, the duration and/or frequency of stimulation required to overcome the Ca^{2+} threshold for secretion should be reduced. We tested this possibility by using a 5 s stimulus that was normally subthreshold for exocytosis. In contrast to the 60 s train, stopping the stimulus after 5 s resulted in little-to-no change in capacitance of DMSO-treated neurons ($n = 8$; Fig. 5*A*, left, *B*). However, the same 5 s stimulus in neurons exposed to 100 nM PMA for 15 min pre-whole-cell to engage Apl Ca_v2 ($n = 7$), resulted in a substantial elevation in capacitance (Fig. 5*A*, middle, *B*). When PKC was activated post-whole-cell, the 5 s stimulus produced a capacitance change similar to control ($n = 12$; Fig. 5*A*, right, *B*).

After the fast-phase of the afterdischarge, action potential frequency falls to ~1 Hz for up to 30 min (Kupfermann and Kandel, 1970). To verify whether a slow-phase-like pattern would reach the Ca^{2+} threshold for secretion, we looked at the effectiveness of a long (10 min) 1 Hz train of 75 ms depolarizing steps from −80 to 0 mV to change capacitance. As this train is protracted, the development of exocytosis was measured by monitoring capacitance approximately every 10 s for ~1 s periods. In DMSO ($n = 7$), neurons presented a minimal capacitance response for the

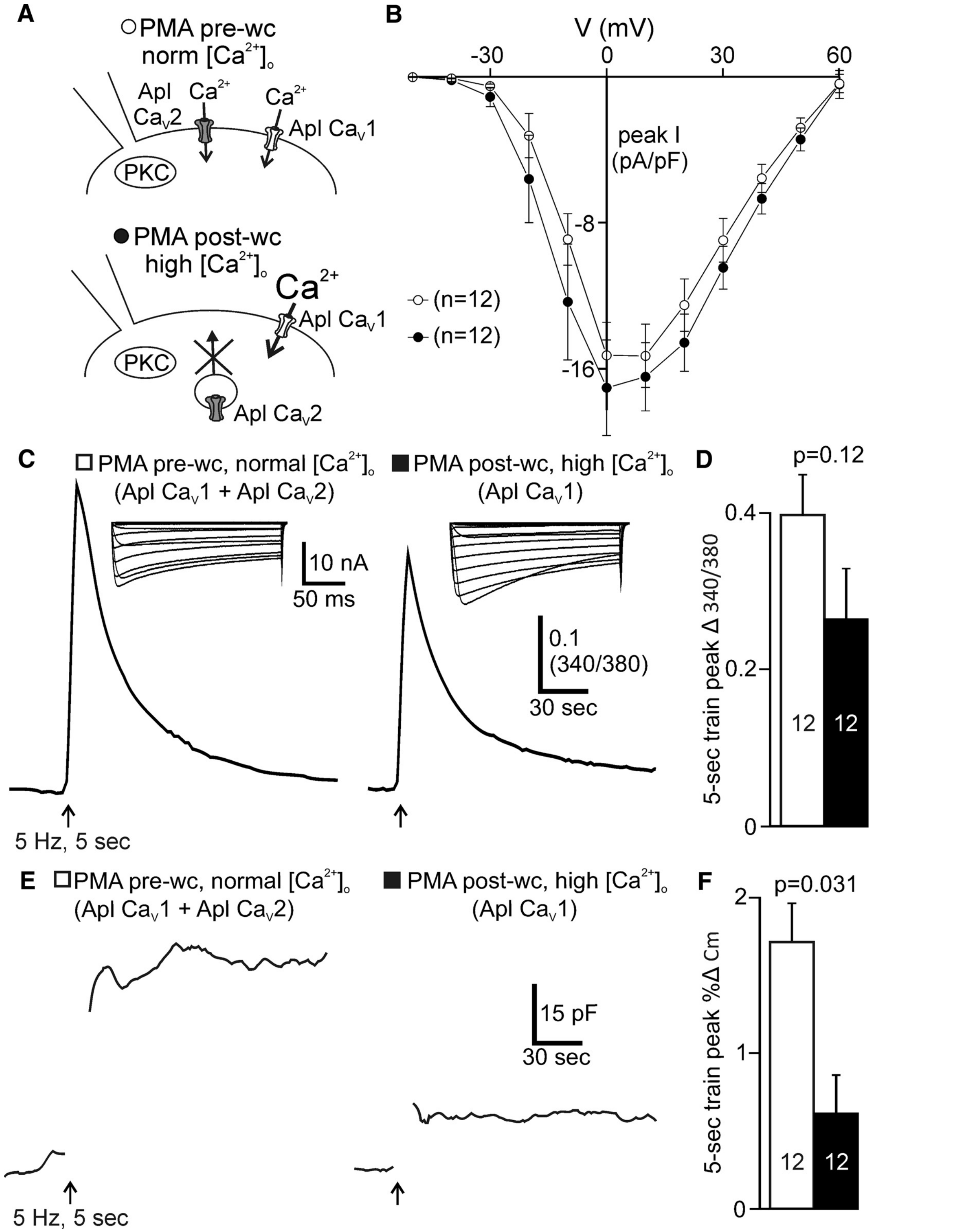

Figure 6. The insertion of Apl Ca_v2 channels increases the strength of excitation-secretion coupling. ***A***, To mimic the enhancement of Ca^{2+} current by Apl Ca_v2 insertion (top, PMA pre-whole-cell), basal Apl Ca_v1 Ca^{2+} current (bottom, PMA post-whole-cell) is enhanced by bathing neurons in a high-Ca^{2+} external solution (16.5 mM Ca^{2+}; equi-molar substitution of Ca^{2+} for Mg^{2+}). ***B***, Cells treated with 100 nM PMA post-whole-cell immersed in high external Ca^{2+} show large current that is not significantly different from neurons recorded in normal Ca^{2+} (11 mM) and provided with PMA pre-whole-cell (all voltages unpaired Student's *t* test). All subsequent Ca^{2+} imaging and capacitance tracking data are acquired from these control and test groups. ***C***, After incubation with PMA post-whole-cell (right), a 5 Hz, 5 s train of 75 ms pulses from −80 to 0 mV in high Ca^{2+} produces a Ca^{2+} signal only slightly smaller than that of neurons in normal Ca^{2+} with Apl Ca_v2 recruitment due to PMA pre-whole-cell (left). Insets, Whole-cell Ca^{2+} current, elicited as per Figure 1*C*, acquired from those neurons selected for display of train Ca^{2+} signals. ***D***, Summary data show that the peak change in 340/380 during the 5 s train is not significantly different between PMA pre-whole-cell in normal Ca^{2+} and PMA post-whole-cell in high Ca^{2+} (unpaired Student's *t* test). ***E***, Capacitance tracking taken simultaneously with the intracellular Ca^{2+} measurements from cells presented in ***C***. In a neuron given PMA post-whole-cell and bathed in high Ca^{2+} (right), the 5 s train evokes only a small rise in capacitance compared with a cell in normal Ca^{2+} and treated with PMA pre-whole-cell (left). ***F***, The mean peak percentage change in membrane capacitance following the 5 s train between the two conditions is significant (unpaired Student's *t* test).

duration of the 10 min train (Fig. 5*C*, left, *D*). By contrast, initiating the train in neurons provided 100 nM PMA pre-whole-cell for 15 min ($n = 10$), produced an increase in capacitance within 10–20 s, which plateaued by the end of the stimulus (Fig. 5*C*, middle, *D*). Neurons exposed to PMA post-whole-cell ($n = 7$), to engage PKC in the absence of Apl Ca_v2, showed only a small elevation in capacitance during the 10 min train (Fig. 5*C*, right, *D*).

The insertion of Apl Ca_v2 increases excitation-secretion coupling

Because of its profound impact on secretion, we investigated whether Apl Ca_v2 insertion strengthens the efficacy of excitation-secretion coupling. To first control for the fact that Ca^{2+} current from cells using both Apl Ca_v2 and Apl Ca_v1 are larger than current from cells using only Apl Ca_v1, the latter were amplified by elevating extracellular Ca^{2+} (Fig. 6*A*). Cells bathed in normal external Ca^{2+} (11 mM) and given PMA pre-whole-cell to marshal Apl Ca_v2 ($n = 12$) exhibited large Ca^{2+} current that was not significantly different from cells in high-Ca^{2+} external (16.5 mM) and given 100 nM PMA post-whole-cell ($n = 12$; Fig. 6*B*). Because PKC was active in both cases, ostensibly, the only difference between these two groups was the presence of functional Apl Ca_v2 at the membrane.

If enhancing Ca^{2+} influx through Apl Ca_v1 fails to result in the same level of release as a combination of Apl Ca_v1 and Apl Ca_v2, it would suggest that Apl Ca_v2 increases coupling to secretion. Therefore, these neurons were tested for the efficacy of the 5 Hz, 5 s train to elicit Ca^{2+} changes and exocytosis. The peak intracellular Ca^{2+} rise during the 5 s train in neurons with Apl Ca_v1 and recruited Apl Ca_v2 channels (PMA pre-whole-cell) in normal Ca^{2+} ($n = 12$) were only slightly larger, and not statistically different from cells using only Apl Ca_v1 channels (PMA post-whole-cell) in high Ca^{2+} ($n = 12$; Fig. 6*C*,*D*). However, even with similar Ca^{2+} current and influx, exocytosis was markedly different between conditions. Large capacitance responses were evoked by the 5 s train in neurons using Apl Ca_v1 and Apl Ca_v2 (PMA pre-whole-cell; $n = 12$; Fig. 6*E*, left). Conversely, neurons using only Apl Ca_v1 (PMA post-whole-cell) in high Ca^{2+} ($n = 12$) displayed minimal exocytosis resembling that in standard Ca^{2+} conditions (Fig. 6*E*, right, *F*).

High-external Ca^{2+} can inhibit PKC signaling in other systems (Kobayashi et al., 1988). Thus, it may be possible that secretion was smaller in the high-Ca^{2+} simply because PMA was unable to elicit PKC-dependent processes (independent of Apl Ca_v2 engagement). This was ruled out by assessing whether high-Ca^{2+} external can occlude the enhancement of train-evoked secretion by PMA. Even in the presence of high-Ca^{2+} external, PMA pre-whole-cell ($\%\Delta\ C_m = 2.00 \pm 0.51$) significantly increased 5 s train-evoked secretion relative to cells exposed to DMSO ($\%\Delta\ C_m = 0.50 \pm 0.41$) or PMA post-whole-cell ($\%\Delta\ C_m = 0.74 \pm 0.34$; $H = 9.5$, $df = 2$, $p = 0.0090$, KW one-way ANOVA; DMSO vs PMA pre-whole-cell, $p < 0.05$; DMSO vs PMA post-whole-cell, $p > 0.05$; PMA pre-whole-cell vs PMA post-whole-cell $p < 0.05$; Dunn's multiple-comparisons test).

Dissociation of Apl Ca_v2 from train-evoked secretion in cohorts of silent bag cell neurons

The coupling of voltage-gated Ca^{2+} influx to secretion undergoes both developmental and state-dependent changes (Elhamdani et al., 1998; Fedchyshyn and Wang, 2005). As reproduction in *Aplysia* is a developmentally and seasonally regulated behavior (Berryl., 1982; Nick et al., 1996a,b), similar variations may occur in the bag cell neurons, possibly by altering Apl Ca_v1 activity, Apl Ca_v2 insertion by PKC, or the coupling of Apl Ca_v2 to secretion. Animals that are not laying eggs yield bag cell neurons that show very low levels of secretion in response to Apl Ca_v1 Ca^{2+} current during the fast-phase-like 5 Hz, 60 s train (Hickey et al., 2013). In the present study, we designated these neurons as silent, compared with secretory competent cells from reproductively active animals. The underlying cause for this absence of secretion is unknown; therefore, we compared capacitance responses and train Ca^{2+} entry in silent and competent bag cell neurons. In response to a 5 Hz, 60 s train, competent neurons ($n = 13$; reproduced from the dataset depicted in Fig. 1*E*, white bar) exhibited a large rise in membrane capacitance (Fig. 7*A*, left, *C*). Conversely, silent cells (n = 11) presented almost no measurable change in capacitance following the train (Fig. 7*A*, middle, *C*). Moreover, in competent neurons ($n = 13$), the peak somatic Ca^{2+} signal during the train was expectedly large (Fig. 7*B*, left, *D*), whereas silent cells ($n = 11$) showed less robust changes in intracellular Ca^{2+} (Fig. 7*B*, middle, *D*). Furthermore, the resting membrane capacitance of silent neurons used was nearly a fold smaller than competent cells (secreting cohort, $C_m = 746.0 \pm 80.5\ pF$, $n = 13$; silent cohort: C_m: $351.8 \pm 38\ pF$, $n = 19$; $p < 0.0001$, Mann–Whitney *U* test). This aligns with reports in mammals showing that neuroendocrine cells are often markedly smaller during periods of disuse (Lin et al., 1996; de Kock et al., 2003).

In competent cells, Apl Ca_v2 augments Ca^{2+} influx and is strongly coupled to secretion. We tested whether a similar arrangement is present in silent neurons by engaging Apl Ca_v2 in an attempt to rescue train-evoked exocytosis. However, a 15 min incubation with 100 nM PMA pre-whole-cell did not confer measurable secretion to the 60 s train ($n = 8$; Fig. 7*A*, right, *C*). Interestingly, the failure of PMA to rescue secretion did not arise from an inability to marshal Apl Ca_v2, as these silent cells showed enhanced Ca^{2+} influx that was nearly equal to that of competent cells which used only Apl Ca_v1 ($n = 8$; Fig. 7*B*, right, *D*).

PKC activation facilitates slow secretion evoked by mitochondrial Ca^{2+} release

The results thus far suggest that PKC enhances train-evoked secretion solely through the recruitment of Apl Ca_v2. This is supported by the fact that PMA has no impact on stimulus-dependent capacitance responses once the insertion of Apl Ca_v2 has been prevented by whole-cell dialysis. To further test for any secondary effects of PKC we measured the impact of PMA on slow sustained secretion triggered by intracellular Ca^{2+} release from mitochondria.

In the bag cell neurons, one of the primary intracellular Ca^{2+} stores is provided by mitochondria, which are implicated in ELH secretion during the afterdischarge (Michel and Wayne, 2002; Geiger and Magoski, 2008; Groten et al., 2013; Hickey et al., 2013). In other neurons, mitochondria localize to regions of transmitter release (Sheng and Cai, 2012). Therefore, we first evaluated the spatial relationship between mitochondria and ELH in cultured bag cell neurons. Neurons were exposed to the vital dye, MitoTracker Red, to label mitochondria, then subsequently fixed and stained with rabbit anti-ELH. Both Mitotracker and ELH staining were abundant in the soma and the primary neurites ($n = 16$; Fig. 8*A*,*B*).

To trigger intracellular Ca^{2+} release from the mitochondria, neurons were exposed to FCCP. This protonophore collapses the mitochondrial membrane potential and liberates stored Ca^{2+} to initiate secretion in bag cell neurons and chromaffin cells (Heytler and Prichard, 1962; Miranda-Ferreira et al., 2009; Hickey et al., 2013). Administering 20 μM FCCP to neurons pro-

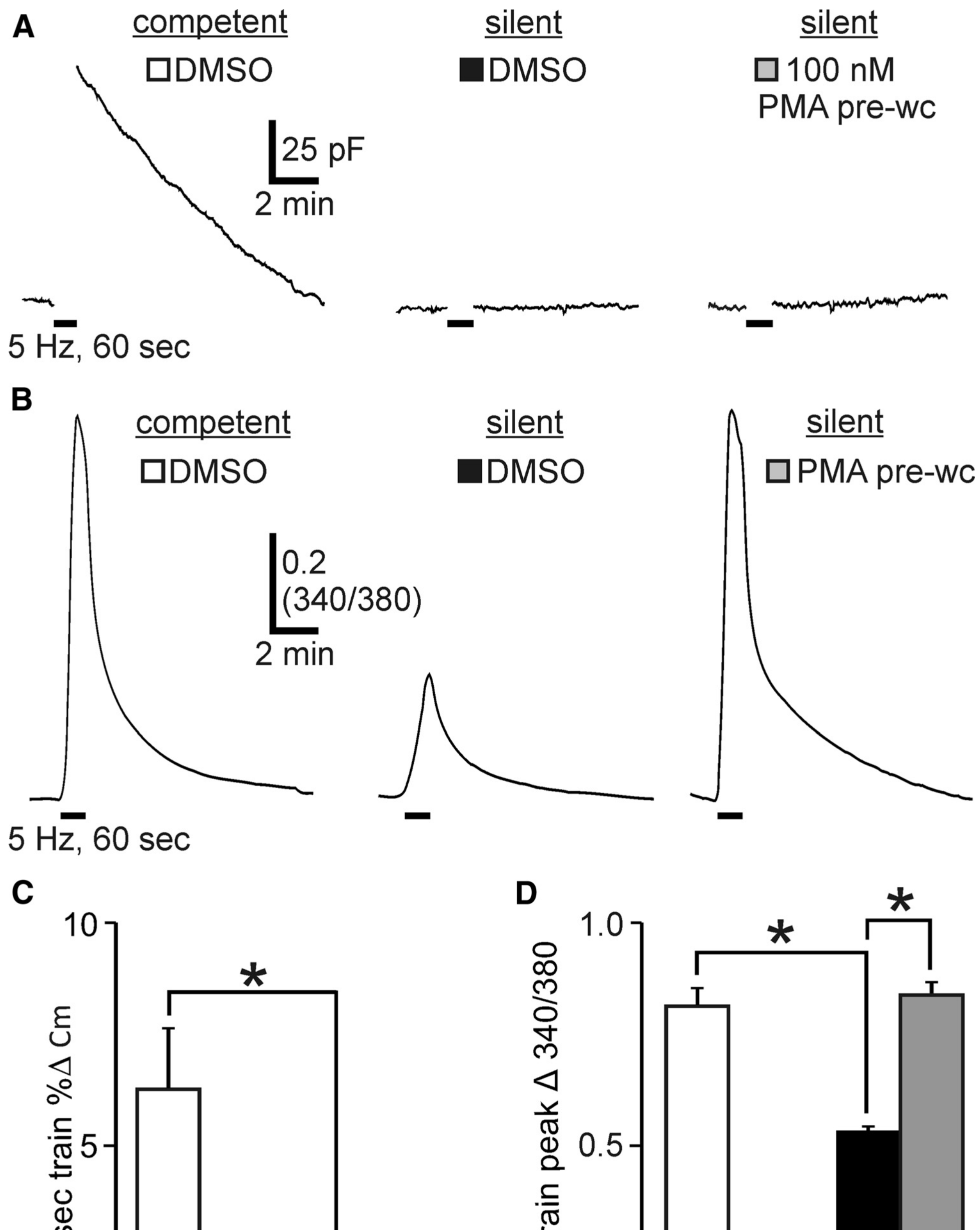

Figure 7. Cohorts of silent bag cell neurons show reduced Apl Ca_v1 Ca^{2+} entry and a disassociation of Apl Ca_v2 activity from train-evoked secretion. ***A***, Left, Most animals yield secretory competent neurons which, following DMSO treatment, demonstrate prominent exocytosis to a 5 Hz, 60 s train of 75 ms pulses from −80 to 0 mV. Middle, Other animals, in which egg-laying behavior is absent, produce secretory silent neuronal cohorts that show essentially no change in capacitance to the 5 Hz, 60 s train, again following DMSO. Right, In a silent neuron, a 15 min treatment with 100 nM PMA pre-whole-cell is ineffective at restoring the train-evoked capacitance response. ***B***, The somatic Ca^{2+} rise during a 60 s train in a silent cell (DMSO; middle) is substantially smaller than in a secreting cell (DMSO; left). PMA pre-whole-cell markedly heightens the peak train Ca^{2+} response in a silent neuron (right). ***C***, Summary data show a significantly smaller train-evoked peak percentage increase in capacitance between competent (DMSO; reproduced from control of Fig. 1) and silent cells in the absence (DMSO) or presence of PMA pre-whole-cell. Moreover in silent cells, PMA exposure pre-whole-cell did not significantly increase capacitance responses relative to DMSO control ($H = 14.8$, df = 2, $p < 0.006$, KW one-way ANOVA; *$p < 0.05$, Dunn's multiple-comparisons test). ***D***, Peak Ca^{2+} rise during the train in DMSO-treated silent cells is significantly smaller than responses measured from secreting cells (DMSO) or silent cells exposed to PMA pre-whole-cell ($H = 8.23$, df = 2, $p < 0.02$, KW one-way ANOVA; *$p < 0.05$, Dunn's multiple-comparisons test).

duced a slow, but substantial rise in somatic Ca^{2+} that was not modified by 100 nM PMA post-whole-cell (control $n = 8$; PMA $n = 7$; Fig. 8*C*). Yet, capacitance responses were strikingly different between the conditions. In control neurons ($n = 13$), FCCP prompted a slow-onset rise in capacitance which typically peaked after several minutes (Fig. 8*D*). Conversely, neurons given PMA post-whole-cell ($n = 9$) showed a larger and more prolonged capacitance response to FCCP (Fig. 8*D*).

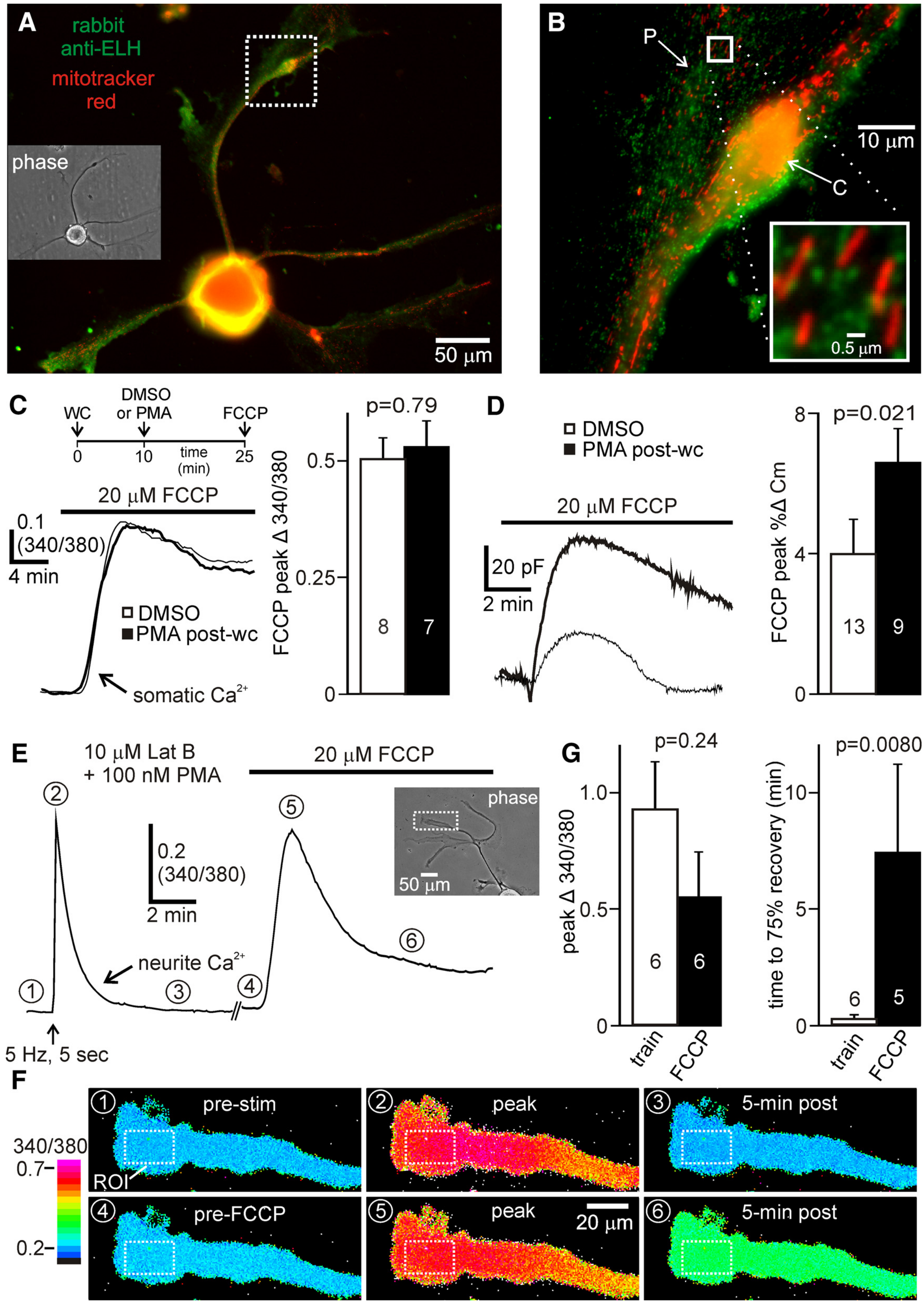

Figure 8. PMA facilitates prolonged secretion triggered by mitochondrial Ca^{2+} release. ***A***, Left, Superimposed images of a fixed cultured bag cell neuron demonstrates the relative distribution of immunolabeled ELH (green; ELH 1° at 1:1000, AlexaFluor 488 2° at 1:200) and mitochondria (MitoTracker Red, 500 nM) in the soma and four primary neurites. Focal planes for all images are optimized to view the neurites. Inset, Phase contrast image of the labeled neuron. The area outlined with the white box is shown in ***B***. ***B***, A distal neurite magnified from ***A*** has a characteristic central domain (C) surrounded by a thin, veil-like peripheral region (P). Inset, Magnification of the peripheral domain shows the apposition of MitoTracker Red and ELH puncta. ***C***, Left, Neurons dialyzed with fura-PE3 and voltage-clamped at −80 mV show a slow-onset, but relatively large and prolonged somatic Ca^{2+} signal following 20 μM FCCP (at bar). Compared with DMSO (light trace), post-whole-cell treatment with 100 nM PMA for ∼15 min (see inset for time line) does not alter the FCCP-induced Ca^{2+} release (dark trace). Right, The peak change in Ca^{2+} to FCCP is not significantly different between DMSO and PMA (unpaired Student's *t* test). ***D***, Left, In DMSO (light trace), capacitance tracking at −80 mV reveals that freeing mitochondrial Ca^{2+} causes a slow and lengthy rise in capacitance which is augmented by PMA post-whole-cell (dark trace). Right, The peak percentage change in capacitance to FCCP is significantly larger (*Figure legend continues.*)

These findings suggest that, unlike secretion triggered by voltage-gated Ca^{2+} entry secretion initiated by mitochondrial Ca^{2+} release is sensitive to PMA post-whole-cell. The difference in PMA-sensitivity may be attributable to differences in the temporal or spatial properties of the Ca^{2+} signals from Apl Ca_v1 channels and mitochondria. Although we have demonstrated the slow kinetics of mitochondrial Ca^{2+} release in the soma, we sought to further characterize these Ca^{2+} signals in the distal neurites, which are amenable to resolving spatio-temporal properties due to their fine structure. To assess the impact of voltage-gated Ca^{2+} entry in the PKC-sensitized state in the absence of Apl Ca_v2 insertion, we recorded from fura-PE3-injected bag cell neurons presented with 100 nM PMA following exposure to 10 μM Lat B. Moreover, we bathed neurons in high-Ca^{2+} nASW to enhance Apl Ca_v1 current, since our results indicate that even under these conditions there is little apparent secretion during a 5 Hz, 5 s train stimulus. After drug application, neurites were imaged while the soma was sharp-electrode current-clamped at −60 mV. A train of action potentials evoked by 5 Hz, 5 s depolarizing current pulses produced a transient rise in Ca^{2+} throughout the most of the primary neurite that quickly returned to baseline after the end of the stimulus (Fig. 8*E*,*F*). Conversely, exposing the same neurons to 20 μM FCCP to liberate mitochondrial Ca^{2+} produced a much slower onset Ca^{2+} response in the same regions of the neurite which lasted substantially longer than the Ca^{2+} signal following the train stimulus (Fig. 8*E*,*F*). While the peak Ca^{2+} signal was not significantly different between the two Ca^{2+} signals, the time to 75% recovery from the peak Ca^{2+} response during FCCP was much longer than the Ca^{2+} signal after the train, and reached the level of significance (Fig. 8*G*).

Discussion

In the present study, we examined the contribution of Apl Ca_v2 to secretion from bag cell neurons. Consistent with other work, we found that prior whole-cell recording occluded the recruitment of Apl Ca_v2, as PMA addition after dialysis had no impact on Ca^{2+} current magnitude or train-evoked somatic Ca^{2+} entry (DeRiemer et al., 1985; Strong et al., 1987). The macroscopic Ca^{2+} current passed by cells possessing either Apl Ca_v1 alone or Apl Ca_v1 plus Apl Ca_v2 showed similar properties, aside from small differences in voltage dependence and voltage-sensitivity of activation.

The finding that Apl Ca_v1 and Apl Ca_v2 macroscopic currents are very similar is consistent with work by others (Strong et al., 1987; Fieber, 1995). Despite these similarities, other electrophysiological and immunocytochemical evidence indicates that these macroscopic currents are carried by distinct channels. Specifically, in association with the PKC-dependent enhancement of macroscopic Ca^{2+} current is the appearance of a larger-conductance single-channel current that is disrupted by patch formation (Strong et al., 1987; Conn et al., 1989b). Moreover, ensemble currents comprised of larger-conductance channels are biophysically similar to the current passed by the smaller-conductance channel (Strong et al., 1987). Last, this study and others have shown that the increase in Ca^{2+} current following PKC activation is sensitive to Lat B, which prevents the trafficking and plasma membrane insertion of the Apl Ca_v2 α-1 subunit (Zhang et al., 2008).

Augmented Ca^{2+} current and influx following Apl Ca_v2 recruitment was associated with a facilitation in the capacitance response triggered by stimuli that mimic the afterdischarge. PKC also increases Ca^{2+} current and facilitates synaptic transmission in *Aplysia* buccal neurons or mammalian central neurons (Fossier et al., 1990, 1994; Swartz et al., 1993; Brody and Yue, 2000). However, unlike these and other forms of facilitation, we show that PKC does so uniquely, by recruiting distinct Ca^{2+} channels to the membrane. The PMA-evoked recruitment of Apl Ca_v2, and ensuing elevation of Ca^{2+} influx and secretion, is prevented by Lat B, which disrupts the polymerization of new actin filaments (Morton et al., 2000). Furthermore, blocking Apl Ca_v2 recruitment by establishing whole-cell configuration before, but not after, engaging PKC, entirely impedes the facilitation of train-induced secretion by PMA. As such, this appears to be principally mediated by Apl Ca_v2 recruitment rather than a mechanism downstream from Ca^{2+} influx, or any PMA-elicited changes in voltage dependence.

The recruitment of Apl Ca_v2 confers substantial secretion to brief or slow-frequency stimuli that were ineffective at reaching the threshold for secretion in cells using Apl Ca_v1 alone. Similar properties have been demonstrated in adrenal chromaffin cells and neurohypophyseal terminals (Seward et al., 1995; Seward and Nowycky, 1996). In these cells, the requisite activity pattern for secretion is not fixed, but relies on a set amount of cumulative Ca^{2+} entry. Thus, greater Ca^{2+} entry per pulse achieves the Ca^{2+} threshold more readily and lowers the frequency and/or duration of activity necessary for secretion.

Ca^{2+} current passed through a combination of Apl Ca_v2 and Apl Ca_v1 channels was more effective at eliciting secretion than equivalent current derived from Apl Ca_v1. These results suggest that Apl Ca_v2 engages secretion more readily than Apl Ca_v1, rather than simply causing a general increase in Ca^{2+} entry. In pancreatic β cells and chromaffin cells, L-type Ca^{2+} channels preferentially trigger secretion by physically colocalizing with secretory vesicles in active zone-like regions (Bokvist et al., 1995; Robinson et al., 1995; Elhamdani et al., 1998). Likewise, the insertion of Apl Ca_v2 channels could create new sites of Ca^{2+} entry that access vesicle populations more readily than Apl Ca_v1. This is compelling, given that in mammalian neurons, Ca_v2 family channels preside over secretion by forming a complex with the SNARE apparatus at active zones (White and Kaczmarek, 1997; Catterall and Few, 2008). Strong et al. (1987) observed possible differences in the distribution of the two channel species in single-channel patches from bag cell neuron somata. Likewise, at distal neurites, PKC expands the lamellapodia and causes Apl Ca_v2 α-1 subunits to translocate to the leading edge, producing new zones of Ca^{2+} entry that are absent with Apl Ca_v1 alone (Knox et al., 1992; Zhang et al., 2008). Such coupling may be advantageous for sus-

←

(*Figure legend continued.*) with PMA post-whole-cell than DMSO (unpaired Student's *t* test). ***E***, Intracellular Ca^{2+} in the distal neurite of a bag cell neuron bathed in high-Ca^{2+} external nASW (16.5 mM Ca^{2+}) while maintaining the soma at −60 mV with sharp-electrode current-clamp. Neurons were treated with 10 μM Lat B for 1 h and then provided PMA for 15 min to activate PKC in the absence of Apl Ca_v2 recruitment. Numbers correspond to images from ***F***. Delivering a 5 Hz, 5 s train of depolarizing current pulses produces a steep rise in Ca^{2+} that rapidly decays to prestimulus levels (***E1***–***E3***). Subsequently, bath application of FCCP, while maintaining membrane voltage at −60 mV, elicits a rise in Ca^{2+} that endures for many minutes (***E4***–***E6***). Inset, Phase image of the bag cell neuron soma and the neurite (white box) presented in ***E*** and ***F***. ***F***, Ratiometric images of emission following 340/380 nm excitation of a bag cell neuron distal neurite quantified in ***E***. Images (***F1***–***F6***) show before, at peak, and 5 min post-peak for the Ca^{2+} responses during either the train stimulus (top) or FCCP (bottom). Dashed box in each image delineates the ROI used to acquire the data. Note that during FCCP Ca^{2+} remains high throughout the neurite even 5 min post-peak. ***G***, Left, The peak change in 340/380 during the 5 Hz, 5 s train stimulus and FCCP are not significantly different (unpaired Mann–Whitney *U* test). Right, The time to 75% recovery from the peak 340/380 response is significantly longer following FCCP than the train (unpaired Mann–Whitney *U* test). The *n* value for FCCP is different in the right panel because one cell did not recover to 75% within the recording period.

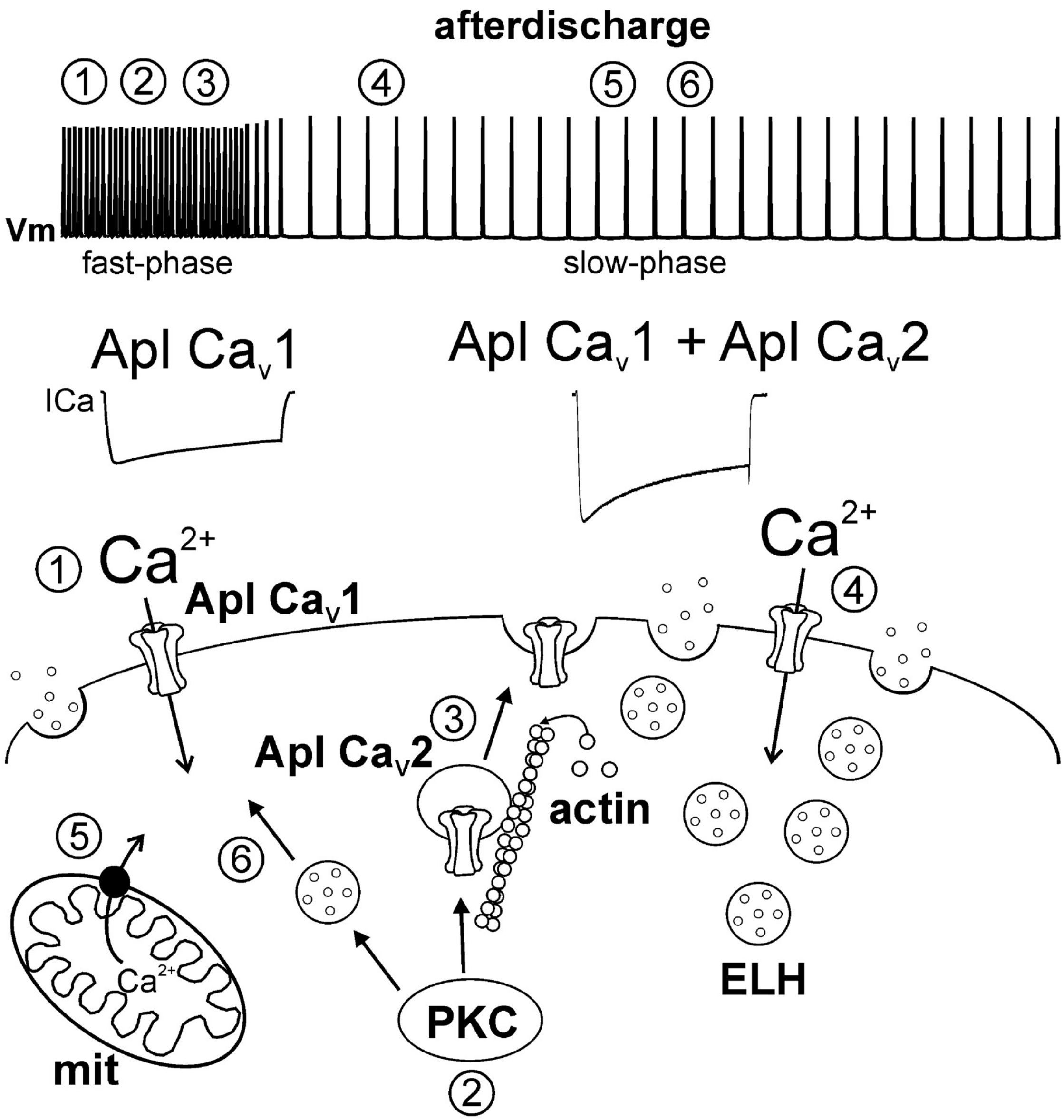

Figure 9. PKC activation during the afterdischarge facilitates peptide release by recruiting Apl Ca_v2 to the membrane and engaging a process downstream from Ca^{2+} influx. A conceptual model for the enhancement of secretion during an afterdischarge by Apl Ca_v2 recruitment, based on the present study and prior work (Strong et al., 1987; Conn et al., 1989a; Wayne et al., 1999; Zhang et al., 2008; White and Magoski, 2012). Top, An idealized bag cell neuron afterdischarge containing an early fast-phase and late slow-phase. Numbers correspond to chronological events portrayed in the illustration. Bottom, ***1***, A brief synaptic input triggers the start of the afterdischarge, during which time Ca^{2+} entry is mediated by Apl Ca_v1 and is loosely coupled to secretion. ***2***, As the afterdischarge progresses PKC is activated. ***3***, PKC causes Apl Ca_v2-containing vesicles to associate with actin and traffic/insert into the plasma membrane via a process requiring the polymerization of new filaments. ***4***, Apl Ca_v2 is present in the membrane and occupies regions which have greater coupling to secretory vesicles than Apl Ca_v1, thereby sustaining peptide release throughout the slow-phase. ***5***, After prolonged Ca^{2+} entry, Ca^{2+} liberated from the mitochondria provide an additional source for secretion. ***6***, PKC also facilitates secretion directly, possibly by making vesicles available for release after prolonged Ca^{2+} changes (such as from the mitochondria).

taining secretion during periods with minimal burst frequency. For example, in the absence of Apl Ca_v2, the slow-phase-like train fails to elicit secretion, despite the majority of ELH release *in vivo* occurring during the slow-phase of the afterdischarge (Loechner et al., 1990; Michel and Wayne, 2002). However, during a genuine afterdischarge, Apl Ca_v2 channels are involved throughout the slow-phase (Conn et al., 1989a,b). Consequently, the insertion of Apl Ca_v2, and the associated enhanced excitation-secretion coupling, may be necessary for sustaining slow-phase secretion and ultimately propagation of the species.

The bag cell neurons show dramatic differences in voltage-gated Ca^{2+} entry and excitation–secretion coupling in relation to reproductive behavior. The absence of secretion is associated with smaller train Ca^{2+} entry through Apl Ca_v1, probably due to reduced Apl Ca_v1 Ca^{2+} current density, which has also been observed in reproductively immature animals (Nick et al., 1996a). In rats, changes to lactating behavior are associated with a similar drop in stimulus-evoked secretion in magnocellular neurons, due in part to smaller voltage-gated Ca^{2+} currents (de Kock et al., 2003). Additionally, the absence of secretion in silent neurons appears to be due to the uncoupling of Ca^{2+} entry from exocytosis. Despite the recovery of substantial train Ca^{2+} entry by recruiting Apl Ca_v2, secretion remains absent. In the calyx of Held and adrenal chromaffin cells, secretion becomes more efficient with development, as the spatial relationship between Ca^{2+} channels and vesicles tightens (Elhamdani et al., 1998; Fedchyshyn and Wang, 2005). Unlike reproductively mature animals, bag cell neurons in juvenile animals show nonpunctate distribution of Apl Ca_v2 α-1 subunits (White et al., 1998). Therefore, Apl Ca_v2 insertion may be mislocalized in relation to peptide vesicles in silent neurons. However, a near lack of secretion in silent neurons implicates other factors, including changes in vesicle class (Nick et al., 1996b), a lower abundance of vesicles (de Kock et al., 2003), or alternate sensors with different Ca^{2+} affinities (Sugita et al., 2002). Nevertheless, our results suggest that the coupling of Apl Ca_v2 to secretion is not fixed, but can differ markedly between animals, possibly to ensure timely reproduction in relation to season and development.

Aside from channel insertion, PKC appears to regulate secretion independent of Ca^{2+} entry, as PMA post-whole-cell enhances capacitance responses triggered by mitochondrial Ca^{2+} release. Interestingly, this secondary effect does not appear to alter secretion initiated by voltage-gated Ca^{2+} entry, because PMA post-whole-cell does not augment capacitance responses to train stimuli. Relative to voltage-gated Ca^{2+} influx, the mitochondrial Ca^{2+} release signal in the neurites/soma persists for a considerable time period; consequently, the secretion is comparatively lengthy. In other cells, PKC facilitates secretion in a delayed fashion by recruiting new vesicles after prior depletion of the readily releasable pool (Nagy et al., 2002). Thus, the secondary influence of PKC may only be detected during prolonged secretion when such processes are engaged, as seen here following mitochondrial Ca^{2+}. If this is the case, then the secondary effect of PKC should become apparent during extended Ca^{2+} influx. Consistent with this, we found that over the 10 min train stimulus, cells exposed to PMA post-whole-cell often presented a small facilitation in secretion despite the disruption of Apl Ca_v2 recruitment. Thus, in addition to recruiting Apl Ca_v2-containing vesicles, PKC promotes secretion directly, possibly by replenishing vesicles after several minutes of ongoing secretion.

By dissecting the contribution of PKC to secretion, we provide strong evidence that the bag cell neurons employ Apl Ca_v2 as a reserve channel that is rapidly recruited to promote peptide release during the afterdischarge (Fig. 9). To our knowledge, this is the first study showing that neurons can employ kinase-dependent Ca^{2+} channel insertion to promptly facilitate the capacity for secretion. This resembles AMPA receptor recruitment during LTP in hippocampal neurons or the insulin-induced insertion of glucose transporters in myocytes. Both forms of insertion rely on fast recruitment of vesicle pools and require actin polymerization (Tong et al., 2001; Gu et al., 2010). Thus, we propose a "presynaptic" equivalent to postsynaptic AMPA receptor insertion for enhancing neuronal communication. Similar forms of plasticity may occur elsewhere; for example, in medullary neurons, the anti-epileptic drug gabapentin, which precludes forward Ca^{2+} channel trafficking (Hendrich et al., 2008; Dolphin, 2012), disrupts the facilitation of glutamate release by PKC (Maneuf and McKnight, 2001). Moreover, during LTP of the perforant pathway-CA1 synapse, formerly uninvolved N-type Ca^{2+} channels are recruited through an undetermined mechanism to enhance the efficacy of synaptic transmission (Ahmed and Siegelbaum, 2009). Our work suggests that dynamic regulation of membrane channel content could be an advantageous form of plasticity. By recruiting additional channels, neurons would be able to stably augment Ca^{2+} influx during periods of prolonged excitability and output, or even transform the spatial pattern of Ca^{2+} entry and produce additional regions of secretion.

References

Acosta-Urquidi J, Dudek FE (1981) Soma spike of neuroendocrine bag cells of *Aplysia.* J Neurobiol 12:367–378. CrossRef Medline

Ahmed MS, Siegelbaum SA (2009) Recruitment of N-type Ca^{2+} channels during LTP enhances low release efficacy of hippocampal CA1 perforant path synapses. Neuron 63:372–385. CrossRef Medline

Arch S (1972) Polypeptide secretion from the isolated parietovisceral ganglion of *Aplysia californica.* J Gen Physiol 59:47–59. CrossRef Medline

Artalejo CR, Adams ME, Fox AP (1994) Three types of Ca^{2+} channel trigger secretion with different efficacies in chromaffin cells. Nature 367:72–76. CrossRef Medline

Bauer CS, Nieto-Rostro M, Rahman W, Tran-Van-Minh A, Ferron L, Douglas L, Kadurin I, Sri Ranjan Y, Fernandez-Alacid L, Millar NS, Dickenson AH, Lujan R, Dolphin AC (2009) The increased trafficking of the calcium channel subunit $\alpha_2\delta$-1 to presynaptic terminals in neuropathic pain is inhibited by the $\alpha_2\delta$ ligand pregabalin. J Neurosci 29:4076–4088. CrossRef Medline

Berry RW (1982) Seasonal modulation of synthesis of the neurosecretory egg-laying hormone of *Aplysia.* J Neurobiol 13:327–335. CrossRef Medline

Bokvist K, Eliasson L, Ammälä C, Renström E, Rorsman P (1995) Co-localization of L-type Ca^{2+} channels and insulin-containing secretory granules and its significance for the initiation of exocytosis in mouse pancreatic β-cells. EMBO J 14:50–57. Medline

Brody DL, Yue DT (2000) Relief of G-protein inhibition of calcium channels and short-term synaptic facilitation in cultured hippocampal neurons. J Neurosci 20:889–898. Medline

Castagna M, Takai Y, Kaibuchi K, Sano K, Kikkawa U, Nishizuka Y (1982) Direct activation of calcium-activated, phospholipid-dependent protein kinase by tumor-promoting phorbol esters. J Biol Chem 257:7847–7851. Medline

Catterall WA (2000) Structure and regulation of voltage-gated Ca^{2+} channels. Annu Rev Cell Dev Biol 16:521–555. CrossRef Medline

Catterall WA, Few AP (2008) Calcium channel regulation and presynaptic plasticity. Neuron 59:882–901. CrossRef Medline

Conn PJ, Strong JA, Azhderian EM, Nairn AC, Greengard P, Kaczmarek LK (1989a) Protein kinase inhibitors selectively block phorbol ester- or forskolin-induced changes in excitability of *Aplysia.* J Neurosci 9:473–479. Medline

Conn PJ, Strong JA, Kaczmarek LK (1989b) Inhibitors of protein kinase C prevent enhancement of calcium current and action potentials in peptidergic neurons of *Aplysia.* J Neurosci 9:480–487. Medline

de Kock CP, Wierda KD, Bosman LW, Min R, Koksma JJ, Mansvelder HD, Verhage M, Brussaard AB (2003) Somatodendritic secretion in oxytocin neurons is upregulated during the female reproductive cycle. J Neurosci 23:2726–2734. Medline

DeRiemer SA, Strong JA, Albert KA, Greengard P, Kaczmarek LK (1985) Enhancement of calcium current in *Aplysia* neurones by phorbol ester and protein kinase C. Nature 313:313–316. CrossRef Medline

Dolphin AC (2012) Calcium channel auxiliary $\alpha_2\delta$- and β subunits: trafficking and one step beyond. Nat Rev Neurosci 13:542–555. CrossRef Medline

Elhamdani A, Zhou Z, Artalejo CR (1998) Timing of dense-core vesicle exocytosis depends on the facilitation L-type Ca^{2+} channel in adrenal chromaffin cells. J Neurosci 18:6230–6240. Medline

Fedchyshyn MJ, Wang LY (2005) Developmental transformation of the release modality at the calyx of Held synapse. J Neurosci 25:4131–4140. CrossRef Medline

Fieber LA (1995) Characterization and modulation of Na^+ and Ca^{2+} currents underlying the action potential in bag cells of two species of *Aplysia.* J Exp Biol 198:2337–2347. Medline

Fossier P, Baux G, Tauc L (1990) Activation of protein kinase C by presynaptic FLRFamide receptors facilitates transmitter release at an *aplysia* cholinergic synapse. Neuron 5:479–486. CrossRef Medline

Fossier P, Baux G, Tauc L (1994) N- and P-type Ca^{2+} channels are involved in acetylcholine release at a neuroneuronal synapse: only the N-type channel is the target of neuromodulators. Proc Natl Acad Sci U S A 91:4771–4775. CrossRef Medline

Frazier WT, Kandel ER, Kupfermann I, Waziri R, Coggeshall RE (1967) Morphological and functional properties of identified neurons in the abdominal ganglion of *Aplysia californica*. J Neurophysiol 30:1288–1351.

Gardam KE, Geiger JE, Hickey CM, Hung AY, Magoski NS (2008) Flufenamic acid affects multiple currents and causes intracellular Ca^{2+} release in *Aplysia* bag cell neurons. J Neurophysiol 100:38–49. CrossRef Medline

Geiger JE, Magoski NS (2008) Ca^{2+}-induced Ca^{2+}-release in *Aplysia* bag cell neurons requires interaction between mitochondrial and endoplasmic reticulum stores. J Neurophysiol 100:24–37. CrossRef Medline

Geiger JE, Hickey CM, Magoski NS (2009) Ca^{2+} entry through a nonselective cation channel in *Aplysia* bag cell neurons. Neuroscience 162:1023–1038. CrossRef Medline

Gillis KD, Mossner R, Neher E (1996) Protein kinase C enhances exocytosis from chromaffin cells by increasing the size of the readily releasable pool of secretory granules. Neuron 16:1209–1220. CrossRef Medline

Groten CJ, Rebane JT, Blohm G, Magoski NS (2013) Separate Ca^{2+} sources are buffered by distinct Ca^{2+} handling systems in *Aplysia* neuroendocrine cells. J Neurosci 33:6476–6491. CrossRef Medline

Grynkiewicz G, Poenie M, Tsien RY (1985) A new generation of Ca^{2+} indicators with greatly improved fluorescence properties. J Biol Chem 260:3440–3450. Medline

Gu J, Lee CW, Fan Y, Komlos D, Tang X, Sun C, Yu K, Hartzell HC, Chen G, Bamburg JR, Zheng JQ (2010) ADF/cofilin-mediated actin dynamics regulate AMPA receptor trafficking during synaptic plasticity. Nat Neurosci 13:1208–1215. CrossRef Medline

Hatcher NG, Sweedler JV (2008) *Aplysia* bag cells function as a distributed neurosecretory network. J Neurophysiol 99:333–343. CrossRef Medline

Hatcher NG, Richmond TA, Rubakhin SS, Sweedler JV (2005) Monitoring activity-dependent peptide release from the CNS using single-bead solid-phase extraction and MALDI TOF MS detection. Anal Chem 77:1580–1587. CrossRef Medline

Hendrich J, Van Minh AT, Heblich F, Nieto-Rostro M, Watschinger K, Striessnig J, Wratten J, Davies A, Dolphin AC (2008) Pharmacological disruption of calcium channel trafficking by the $\alpha 2\delta$ ligand gabapentin. Proc Natl Acad Sci U S A 105:3628–3633. CrossRef Medline

Hendrich J, Bauer CS, Dolphin AC (2012) Chronic pregabalin inhibits synaptic transmission between rat dorsal root ganglion and dorsal horn neurons in culture. Channels 6:124–132. CrossRef Medline

Heytler PG, Prichard WW (1962) A new class of uncoupling agents: carbonyl cyanide phenylhydrazones. Biochem Biophys Res Commun 7:272–275. CrossRef Medline

Hickey CM, Groten CJ, Sham L, Carter CJ, Magoski NS (2013) Voltage-gated Ca^{2+} influx and mitochondrial Ca^{2+} initiate secretion from *Aplysia* neuroendocrine cells. Neuroscience 250:755–772. CrossRef Medline

Hoppa MB, Lana B, Margas W, Dolphin AC, Ryan TA (2012) $\alpha_2\delta$ Expression sets presynaptic calcium channel abundance and release probability. Nature 486:122–125. CrossRef Medline

Hsu SF, Jackson MB (1996) Rapid exocytosis and endocytosis in nerve terminals of the rat posterior pituitary. J Physiol 494:539–553. CrossRef Medline

Hung AY, Magoski NS (2007) Activity-dependent initiation of a prolonged depolarization in *Aplysia* bag cell neurons: role for a cation channel. J Neurophysiol 97:2465–2479. CrossRef Medline

Kaczmarek LK, Finbow M, Revel JP, Strumwasser F (1979) The morphology and coupling of *Aplysia* bag cells within the abdominal ganglion and in cell culture. J Neurobiol 10:535–550. CrossRef Medline

Kaczmarek LK, Jennings KR, Strumwasser F (1982) An early sodium and a late calcium phase in the afterdischarge of peptide-secreting neurons of *Aplysia.* Brain Res 238:105–115. CrossRef Medline

Knox RJ, Quattrocki EA, Connor JA, Kaczmarek LK (1992) Recruitment of Ca^{2+} channels by protein kinase C during rapid formation of putative neuropeptide release sites in isolated *Aplysia* neurons. Neuron 8:883–889. CrossRef Medline

Kobayashi N, Russell J, Lettieri D, Sherwood LM (1988) Regulation of protein kinase C by extracellular calcium in bovine parathyroid cells. Proc Natl Acad Sci U S A 85:4857–4860. CrossRef Medline

Kupfermann I (1967) Stimulation of egg laying: possible neuroendocrine function of bag cells of abdominal ganglion of *Aplysia californica.* Nature 216:814–815. CrossRef Medline

Kupfermann I, Kandel ER (1970) Electrophysiological properties and functional interconnections of two symmetrical neurosecretory clusters (bag cells) in abdominal ganglion of *Aplysia.* J Neurophysiol 33:865–876. Medline

Lin SH, Miyata S, Kawarabayashi T, Nakashima T, Kiyohara T (1996) Hypertrophy of oxytocinergic magnocellular neurons in the hypothalamic supraoptic nucleus from gestation to lactation. Zoolog Sci 13:161–165. CrossRef Medline

Loechner KJ, Azhderian EM, Dreyer R, Kaczmarek LK (1990) Progressive potentiation of peptide release during a neuronal discharge. J Neurophysiol 63:738–744. Medline

Lupinsky DA, Magoski NS (2006) Ca^{2+}-dependent regulation of a nonselective cation channel from *Aplysia* bag cell neurones. J Physiol 575:491–506. CrossRef Medline

Malacombe M, Bader MF, Gasman S (2006) Exocytosis in neuroendocrine cells: new tasks for actin. Biochim Biophys Acta 1763:1175–1183. CrossRef Medline

Man HY, Wang Q, Lu WY, Ju W, Ahmadian G, Liu L, D'Souza S, Wong TP, Taghibiglou C, Lu J, Becker LE, Pei L, Liu F, Wymann MP, MacDonald JF, Wang YT (2003) Activation of PI3-kinase is required for AMPA receptor insertion during LTP of mEPSCs in cultured hippocampal neurons. Neuron 38:611–624. CrossRef Medline

Maneuf YP, McKnight AT (2001) Block by gabapentin of the facilitation of glutamate release from rat trigeminal nucleus following activation of protein kinase C or adenylyl cyclase. Br J Pharmacol 134:237–240. CrossRef Medline

McCleskey EW, Fox AP, Feldman DH, Cruz LJ, Olivera BM, Tsien RW, Yoshikami D (1987) ω Conotoxin: direct and persistent blockade of specific types of calcium channels in neurons but not muscle. Proc Natl Acad Sci U S A 84:4327–4331. CrossRef Medline

Michel S, Wayne NL (2002) Neurohormone secretion persists after post-afterdischarge membrane depolarization and cytosolic calcium elevation in peptidergic neurons in intact nervous tissue. J Neurosci 22:9063–9069. Medline

Miranda-Ferreira R, de Pascual R, Caricati-Neto A, Gandía L, Jurkiewicz A, García AG (2009) Role of the endoplasmic reticulum and mitochondria on quantal catecholamine release from chromaffin cells of control and hypertensive rats. J Pharmacol Exp Ther 329:231–240. CrossRef Medline

Morton WM, Ayscough KR, McLaughlin PJ (2000) Latrunculin alters the actin-monomer subunit interface to prevent polymerization. Nat Cell Biol 2:376–378. CrossRef Medline

Nagy G, Matti U, Nehring RB, Binz T, Rettig J, Neher E, Sørensen JB (2002) Protein kinase C-dependent phosphorylation of synaptosome-associated protein of 25 kDa at Ser187 potentiates vesicle recruitment. J Neurosci 22:9278–9286. Medline

Neher E (1998) Vesicle pools and Ca^{2+} microdomains: new tools for understanding their roles in neurotransmitter release. Neuron 20:389–399. CrossRef Medline

Neher E, Marty A (1982) Discrete changes of cell membrane capacitance observed under conditions of enhanced secretion in bovine adrenal chromaffin cells. Proc Natl Acad Sci U S A 79:6712–6716. CrossRef Medline

Nick TA, Kaczmarek LK, Carew TJ (1996a) Ionic currents underlying developmental regulation of repetitive firing in *Aplysia* bag cell neurons. J Neurosci 16:7583–7598. Medline

Nick TA, Moreira JE, Kaczmarek LK, Carew TJ, Wayne NL (1996b) Developmental dissociation of excitability and secretory ability in *Aplysia* bag cell neurons. J Neurophysiol 76:3351–3359. Medline

Peng YY, Zucker RS (1993) Release of LHRH is linearly related to the time integral of presynaptic Ca^{2+} elevation above a threshold level in bullfrog sympathetic ganglia. Neuron 10:465–473. CrossRef Medline

Pinsker HM, Dudek FE (1977) Bag cell control of egg-laying in freely behaving *Aplysia.* Science 197:490–493. CrossRef Medline

Robinson IM, Finnegan JM, Monck JR, Wightman RM, Fernandez JM (1995) Colocalization of calcium entry and exocytotic release sites in adrenal chromaffin cells. Proc Natl Acad Sci U S A 92:2474–2478. CrossRef Medline

Seward EP, Nowycky MC (1996) Kinetics of stimulus-coupled secretion in dialyzed bovine chromaffin cells in response to trains of depolarizing pulses. J Neurosci 16:553–562. Medline

Seward EP, Chernevskaya NI, Nowycky MC (1995) Exocytosis in peptidergic nerve terminals exhibits two calcium-sensitive phases during pulsatile calcium entry. J Neurosci 15:3390–3399. Medline

Sheng J, He L, Zheng H, Xue L, Luo F, Shin W, Sun T, Kuner T, Yue DT, Wu LG (2012) Calcium-channel number critically influences synaptic strength and plasticity at the active zone. Nat Neurosci 15:998–1006. CrossRef Medline

Sheng ZH, Cai Q (2012) Mitochondrial transport in neurons: impact on synaptic homeostasis and neurodegeneration. Nat Rev Neurosci 13:77–93. CrossRef Medline

Soldo BL, Giovannucci DR, Stuenkel EL, Moises HC (2004) Ca^{2+} and frequency dependence of exocytosis in isolated somata of magnocellular supraoptic neurones of the rat hypothalamus. J Physiol 555:699–711. CrossRef Medline

Sossin WS, Diaz-Arrastia R, Schwartz JH (1993) Characterization of two isoforms of protein kinase C in the nervous system of *Aplysia californica.* J Biol Chem 268:5763–5768. Medline

Strong JA, Fox AP, Tsien RW, Kaczmarek LK (1987) Stimulation of protein kinase C recruits covert calcium channels in *Aplysia* bag cell neurons. Nature 325:714–717. CrossRef Medline

Sugita S, Shin OH, Han W, Lao Y, Südhof TC (2002) Synaptotagmins form a hierarchy of exocytotic Ca^{2+} sensors with distinct Ca^{2+} affinities. EMBO J 21:270–280. CrossRef Medline

Swartz KJ, Merritt A, Bean BP, Lovinger DM (1993) Protein kinase C modulates glutamate receptor inhibition of Ca2+ channels and synaptic transmission. Nature 361:165–168. CrossRef Medline

Tai C, Hines DJ, Choi HB, MacVicar BA (2011) Plasma membrane insertion of TRPC5 channels contributes to the cholinergic plateau potential in hippocampal CA1 pyramidal neurons. Hippocampus 21:958–967. CrossRef Medline

Tam AK, Geiger JE, Hung AY, Groten CJ, Magoski NS (2009) Persistent Ca^{2+} current contributes to a prolonged depolarization in *Aplysia* bag cell neurons. J Neurophysiol 102:3753–3765. CrossRef Medline

Tam AK, Gardam KE, Lamb S, Kachoei BA, Magoski NS (2011) Role for protein kinase C in controlling *Aplysia* bag cell neuron excitability. Neuroscience 179:41–55. CrossRef Medline

Thomas P, Wong JG, Lee AK, Almers W (1993) A low affinity Ca^{2+} receptor controls the final steps in peptide secretion from pituitary melanotrophs. Neuron 11:93–104. CrossRef Medline

Tong P, Khayat ZA, Huang C, Patel N, Ueyama A, Klip A (2001) Insulin-induced cortical actin remodeling promotes GLUT4 insertion at muscle cell membrane ruffles. J Clin Invest 108:371–381. CrossRef Medline

Wayne NL, Lee W, Kim YJ (1999) Persistent activation of calcium-activated and calcium-independent protein kinase C in response to electrical afterdischarge from peptidergic neurons of *Aplysia.* Brain Res 834:211–213. CrossRef Medline

White BH, Kaczmarek LK (1997) Identification of a vesicular pool of calcium channels in the bag cell neurons of *Aplysia californica.* J Neurosci 17:1582–1595. Medline

White BH, Nick TA, Carew TJ, Kaczmarek LK (1998) Protein kinase C regulates a vesicular class of calcium channels in the bag cell neurons of *Aplysia.* J Neurophysiol 80:2514–2520. Medline

White SH, Magoski NS (2012) Acetylcholine-evoked afterdischarge in *Aplysia* bag cell neurons. J Neurophysiol 107:2672–2685. CrossRef Medline

Yang Y, Udayasankar S, Dunning J, Chen P, Gillis KD (2002) A highly Ca^{2+}-sensitive pool of vesicles is regulated by protein kinase C in adrenal chromaffin cells. Proc Natl Acad Sci U S A 99:17060–17065. CrossRef Medline

Zhang Y, Magoski NS, Kaczmarek LK (2002) Prolonged activation of Ca^{2+}-activated K^+ current contributes to the long-lasting refractory period of *Aplysia* bag cell neurons. J Neurosci 22:10134–10141. Medline

Zhang Y, Helm JS, Senatore A, Spafford JD, Kaczmarek LK, Jonas EA (2008) PKC-induced intracellular trafficking of Ca_v2 precedes its rapid recruitment to the plasma membrane. J Neurosci 28:2601–2612. CrossRef Medline

Zhu H, Hille B, Xu T (2002) Sensitization of regulated exocytosis by protein kinase C. Proc Natl Acad Sci U S A 99:17055–17059. CrossRef Medline